NAIST-IS-DD0761201

Doctoral Dissertation

Grasp Effort Evaluation Based on Tendon Force Estimation

Atsutoshi Ikeda

June 25, 2010

Department of Information Systems
Graduate School of Information Science
Nara Institute of Science and Technology

A Doctoral Dissertation
submitted to Graduate School of Information Science,
Nara Institute of Science and Technology
in partial fulfillment of the requirements for the degree of
Doctor of ENGINEERING

Atsutoshi Ikeda

Thesis Committee:

Professor Tsukasa Ogasawara	(Supervisor)
Professor Hirokazu Nishitani	(Co-supervisor)
Associate Professor Jun Takamatsu	(Co-supervisor)
Assistant Professor Yuichi Kurita	(Co-supervisor)

Grasp Effort Evaluation Based on Tendon Force Estimation*

Atsutoshi Ikeda

Abstract

The quantitative evaluation of product usability as well as a specification and a cost is important to product design. Most products e.g. a digital camera, a remote control, a cell-phone have a holding part and a operation part by hands. A grasp effort that is feeling when an user grasps, control and pick up a product is important to product usability. Demands of product design that is reflected a grasp effort are increased. However, quantitative evaluation of sensibility is difficult. A questionnaire survey using a semantic differential method is commonly used for such an evaluation.

This thesis proposes evaluation method of grasp effort based on tendon force estimation for a product usability evaluation system. The aim of this thesis is that to clarify the relationship between the tendon force and human sensation when grasping an object. The proposed method focuses on the force of tendons which are connected to the muscles. The tendon force is calculated based on grasping information (contact points and contact forces) that is measured from a simulator or a robot hand that is equipped with multiple sensors. The grasp effort is estimated quantitatively from the calculated tendon force.

At first of this thesis, the human pinching motion is measured to describe that the tendon force well reflect the human sensation. Since we can not measure the tendon force of human directly, we measure the surface EMG (electromyogram) instead of the tendon force and compare the surface EMG with the questionnaire results in the human experiment. Second, we describe the detail of the proposed

*Doctoral Dissertation, Department of Information Systems, Graduate School of Information Science, Nara Institute of Science and Technology, NAIST-IS-DD0761201, June 25, 2010.

evaluation method of the tendon force margin and explain the tendon force margin. We also explain the grasp force control method based on contact surface eccentricity during the incipient slip. The finger posture and the tendon force margin are calculated using the tendon skeletal model that is constructed from human moment arm data. The pinching motion that is evaluated by a simulation using the proposed evaluation method is compared with human experimental results. As an application, we show the evaluation results of pushing the cell-phone button. Finally, an application for robot hand that is developed as a sensing hand prototype is shown. The motor torques and the human muscle activity are compared in a pinching experiment using the tendon-driven robot hand.

Keywords:

product evaluation, tendon force estimation, grasp force control, tendon skeletal model, robot hand

腱張力推定による持ちやすさ評価*

池田 篤俊

内容梗概

製品設計を評価するには物理的なスペックやコストに加えて見た目や使いやすさなどの感性評価が重要な項目となる．ドアのノブ，リモコン，デジカメなど人が使う製品のほとんどには手で持ったり操作したりするための部位や機能形状が備わっている．人が製品を持ったり操作したりする時に感じる “持ちやすさ” という感覚はユーザが製品のイメージを決める際に大きなウェイトを占めていると考えられる．製品の持ちやすさを設計にフィードバックしたいというニーズが高まっているが感性評価は定量的に扱うことが難しく，従来はSD 法を用いたアンケート評価などの定性的な解析が一般的であった．

本研究では製品評価システムに向けた腱張力余裕度に基づく持ちやすさ評価手法を提案する．製品の把持や操作時の腱張力を推定することにより，製品の使いやすさ評価に利用する．提案手法では筋肉に接続されている腱にかかる負荷である腱張力に着目し，動力学シミュレータから得られた把持データを基に腱骨格モデルによって腱張力を計算し，計算された腱張力から製品の生体力学的な持ちやすさを定量的に評価する．

はじめに腱張力が人の主観評価に影響を与えていることを示すために被験者によるつまみ動作を計測する．人の腱張力は直接計測不可能なため，実験では筋電値を腱張力と等価な情報として計測し，主観評価の方法として従来から用いられているアンケート評価との比較を行う．次に提案手法の詳細を示し，腱張力余裕度について説明する．物体の重量や摩擦係数などの接触情報から初期滑り状態に基づく把持力制御手法を説明する．人のデータを用いた腱骨格モデルについて説明し，指姿勢と腱張力余裕度の計算方法を示す．提案手法を用いてつまみ動作のシミュレーションを行い，被験者の実験結果と比較し提案手法の有効性を示す．また，製品の使いやすさ定量評価の例として，提案手法を用いた携帯電話のボタ

*奈良先端科学技術大学院大学 情報科学研究科 情報システム学専攻 博士論文, NAIST-IS-DD0761201, 2010年6月25日.

ン操作の評価を行う．最後に提案手法の応用例として腱張力を直接計測し製品の持ちやすさ評価に利用できるセンサハンドのコンセプトを提案し，プロトタイプの製作と実験を行う．ロボットハンドを駆動するモータのトルクと人間の筋電値を比較し，ロボットハンドの有効性を示す.

キーワード

製品評価, 腱張力推定, 把持力制御, 腱骨格モデル, ロボットハンド

Contents

List of Figures

List of Tables

Chapter 1

Introduction

1.1 Background

The manufacturing process is improved with the progress of the information technology: CAD (computer aided design), CAE (computer aided engineering), CAM (computer aided manufacturing) and the robot technology: NC (numerical control), Industrial robot. The robot technology mainly contributes to an automation of a production line and a saving cost of labor cost in the production. Fig. 1.1 shows an outline of the manufacturing and coverage of the information technology and the robot technology. These technologies are called "Digital engineering," and they contribute mass production and save the products' cost. Coverage of the robot technology application is smaller than we expect. We aim at expanding the application of the robot technology for helping the product design.

Most industrial robots are suitable for a simple assembly [1] [2] [3]. Japanese industrial standards committee classifies robots into followings [4].

- Sequence control robot
- Playback robot
- Numerically controlled robot
- Intelligent robot
- Sensory controlled robot
- Adaptive controlled robot
- Learning controlled robot
- Teleoperated robot

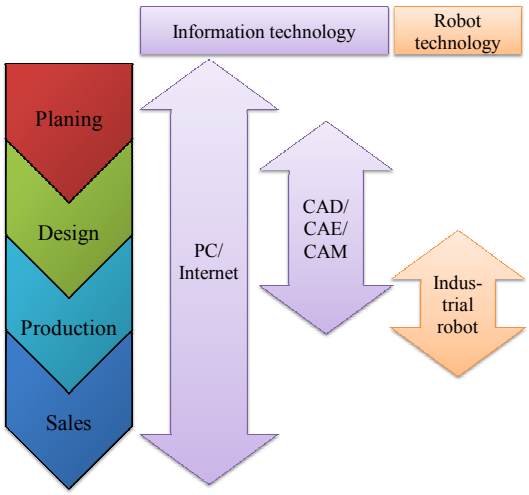

Figure 1.1. Manufacturing flow with typical technologies

Industrial robots are the sequence control robot or the playback robot or the numerically controlled robot or the sensory controlled robot or the teleoperated robot. In addition, few robots are developed for realizing complicated tasks based on the intelligent, the adaptive control and the learning control. However, the aim of these robots is production automation and productivity enhancement.

The human like controlled robot is proposed as one of a new direction of robotics: for example, prosthetic hand, prosthetic leg and actroid. Our study has same direction of the human like controlled robot.

1.2 Research purpose and approach

The aim of this thesis is to design systems for grasp effort evaluation using a simulation. Fig. 1.2 shows the concept of the evaluation system, which is designed to correlate the obtained sensor data with human sensory information.

The quantitative evaluation of product usability is important to product design as well as a specification and a cost. Because customers think that usability of the product is important when they buy the product. Product usability is based on experience and sensation e.g. vision, audition and touch. Many studies discussed about relationship between usability evaluation and human sensation (see in Chapter 2). E.g. vision information effect size-weight illusion, audition

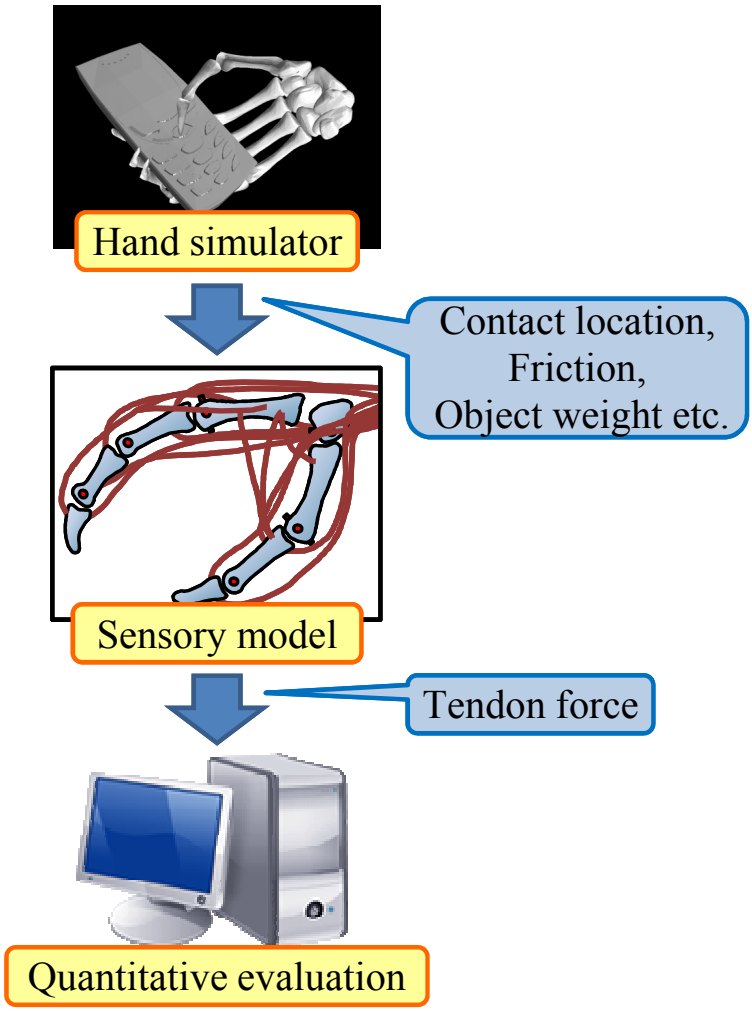

Figure 1.2. Concept of evaluation system

information is used to detect object contact and touch information is used to control of grasp force. Especially, the deep sensation which is one of the touch sensation was focused to evaluate of product usability by following reason, 1. the deep sensation is based on actual load of a product, 2. the deep sensation can do simplified evaluation by using the surface EMG. However, the surface EMG is not stable and it is difficult to measure each muscle independently.

In this thesis, all tendon forces of the index finger and the thumb are calculated using the tendon skeletal model. The product usability is evaluated based on the

tendon forces. The proposed method is more accurate and easy evaluation than using the surface EMG.

The approach of this thesis has 3 steps. First, we show that the surface EMG well reflect human feeling during the pinching motion by human experiment. In this thesis, we focus on the tendon force that is one of the deep sensation (detail of the deep sensation is explained in chapter 2). In the human experiment, we measure the surface EMG (electromyogram) instead of the tendon force. The surface EMG is compared with the questionnaire result that is assumed human feeling.

Second, we explain the grasp effort evaluation. We propose two methods that are a vision based grasp force control and a finger posture estimation using the tendon force margin. The grasp force control method is based on the incipient slip information of the fingertip. The grasp force is calculated from friction and weight of an object. The tendon forces are calculated from the grasp force using the finger models. The index finger and thumb models mimic human tendon skeletal structure. The grasp effort score is defined by the calculated tendon force.

Third, the grasp effort in the case of pinching a cylinder is simulated by the proposed method. The score is compared with the questionnaire evaluation of human experiment. The simulation results show that the simulation scores are similar to the questionnaire survey results and the estimated finger posture is also similar to the human finger posture. We also evaluate the button layouts of the cell-phone. The standard button layout, which is commonly used in the commercial cell-phone is compared with another layout where the pitch is wider. This comparison clarifies that the standard layout is better than the wide layout.

Finally, we develop a prototype of a sensing hand that can measure the tendon force of fingers using a tendon-driven hand model. The motor torque of the tendon-driven robot hand can be assumed to represent the human muscle activity. These results show that the proposed evaluation method can be use for the quantitative evaluation of the product usability.

The contributions of this thesis are:

- Development of the grasp effort evaluation system using the tendon force margin.

- Proposal of the vision based grasp force control method and the finger posture estimation method using the tendon force margin.
- Indication of the tendon force importance to evaluate grasp effort by three approaches that human, simulation and robot hand experiment.

1.3 Thesis outline

This thesis proceeds as follows:

Chapter 1: Introduction
has presented the background, aim, approach, and outline of this thesis.

Chapter 2: Related work
introduces the related works about quantitative evaluation of product usability. These research methods addresses quantitative evaluation via physical restraint without human sensation. This chapter also introduces some research about grasping analysis and musculoskeletal model, because our method is inspired from biomechanical analysis. These research indicate importance of the human sensation based on the receptor reaction for product usability evaluation.

Chapter 3: Human pinching experiment
examines the measurement of the human pinching motion. This chapter show the surface EMG (electromyography), the pinching forces, the questionnaire results and the finger posture during pinching a cylinder. The surface EMG is compared with the questionnaire result that is assumed human feeling.

Chapter 4: Tendon force margin estimation method
explains the detail of the evaluation method of the grasp effort. In this chapter, the grasp force control method and the finger posture estimation method are proposed. It also presents the tendon skeletal finger model of the index finger and the thumb.

Chapter 5: Grasp effort evaluation via simulation
demonstrates the pinching experiment via simulation. We compare the sim-

ulation results with the human experimental results. It also demonstrates the evaluation of the cell-phone button layout.

Chapter 6: Grasp effort evaluation using robot finger

demonstrates the pinching experiment via a robot finger. We compare the experimental results using a robot finger with the human experimental results.

Chapter 6: Conclusion and Future work

concludes this thesis, and gives the directions of future works.

Chapter 2

Related work

This chapter shows relevant studies of the product usability evaluation. In recent years, quantitative evaluation methods have been proposed based on physical data that are measured by sensors. These studies addressed the quantitative evaluation of a power grasp using the whole hand (palm and fingers). At first, we introduce previous grasp effort evaluation methods. Next, studies of human grasping analysis are described. Finally, human models that are produced in biomechanics and robotics are shown.

2.1 Quantitative evaluation of grasping an object

A questionnaire survey using a semantic differential method is commonly used for grasp effort evaluation. However, a questionnaire survey takes many subject and a lot of time for an experiment. The quantitative evaluation of the grasp effort is difficult because the grasp effort is based on users feeling and perception. It is complex problem to measure user feeling and perception with sensors.

On the other hand, the grasping is evaluated from a viewpoint of physical restraint. The most useful grasp restraint are the form closure and the force closure [5]. These names were used in the field of Mechatronics and Robotics over 100 years ago. Some research propose a system of the grasp effort evaluation utilizing these condition. Endo *et al.* develop a simulator that can evaluate stability and ease of a person grasping a handheld product without real subjects and physical objects [6]. Fig. 2.1 shows the overview of grasping assessment system that Endo *et al.* proposed. Sugiyama *et al.* proposed a grasp criterion that yields the best grasping position for a robot hand with two soft fingers [7]. Grasp It! is a grasp data base and a tool for both grasp planning and benchmarking [8] [9]. Fig. 2.2 shows hand postures that are calculated using the Grasp It!. However, these studies were not considered human sensory function.

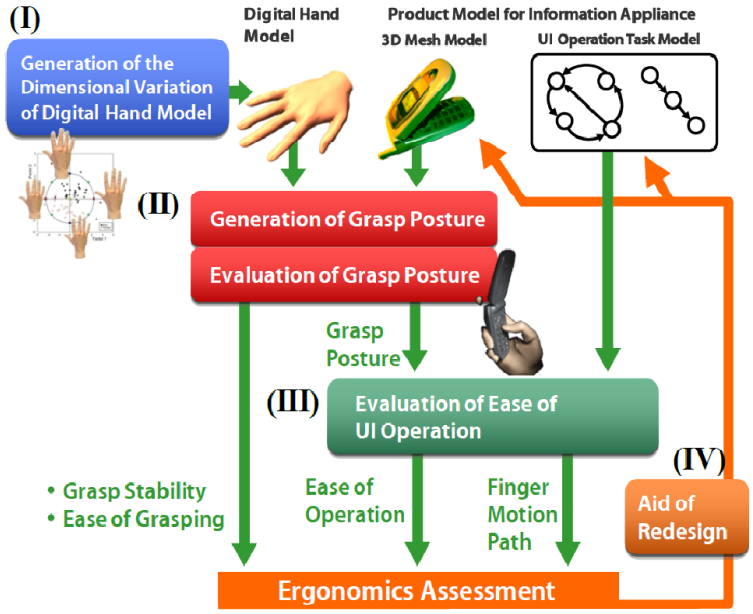

Figure 2.1. The overview of grasping assessment system [6]

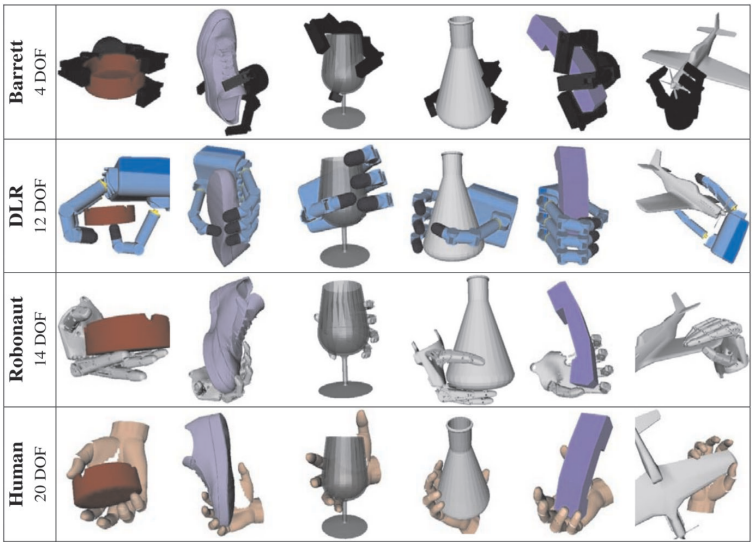

Figure 2.2. Best hand postures were calculated by Grasp It! [8]

2.2 Grasping analysis

The influence of human sensations for Grasp object

Many human sensations (memory, visual, sound and haptics) are important for an object grasp and manipulation. Flanagan *et al.* discussed the importance of "contact events" in the control of manipulation tasks and the importance of predictive control mechanisms that are based on knowledge of object properties (fig. 2.3) [10]. Terabayashi *et al.* discussed about effect of visual size of hand and visual time delay for grasp strategy [11]. Gordon *et al.* indicated that motor commands used to lift commonly handled objects were scaled before the lifting movement based on visual identification of an object and a fairly accurate estimate of the object's weight [12].

Haptic information is one of the most important sensation for an object grasp and manipulation. Human receives the haptic information from somatic sensation organ. There are two groups, the cutaneous sensation and the deep sensation. The cutaneous sensation arise from the receptors under the skin. The deep sensation arise from the receptors in muscles and the tendons.

Cutaneous sensation analysis

The cutaneous sensation has four kinds of receptors that have different area and reaction speed [13]. Fig. 2.4 shows the sketch of the cutaneous sensation receptors. These receptors are fired according to each response property when grasping an object [14]. Johansson *et al.* examined human pinching motion using the index finger and the thumb under the condition that some weight and friction [15] [16]. These results indicate that human pinches an object using $1.2 \sim 1.4$ times force of minimum force that needs to lift up an object. The cutaneous sensation are required by human pinching force control. Especially, the incipient slip information in early slip phase is important for the force control [17].

On the other hand, for the purpose of achieving robotic grasping inspired from human tactile sensation, a number of tactile sensors have been developed. Maekawa *et al.* developed a finger-shaped sensor by which the contact point of the fingertip can be measured[18]. Ferrier *et al.* presented a reconstruction method of the shape of a deformable membrane from the camera image[19]. Howe *et al.*

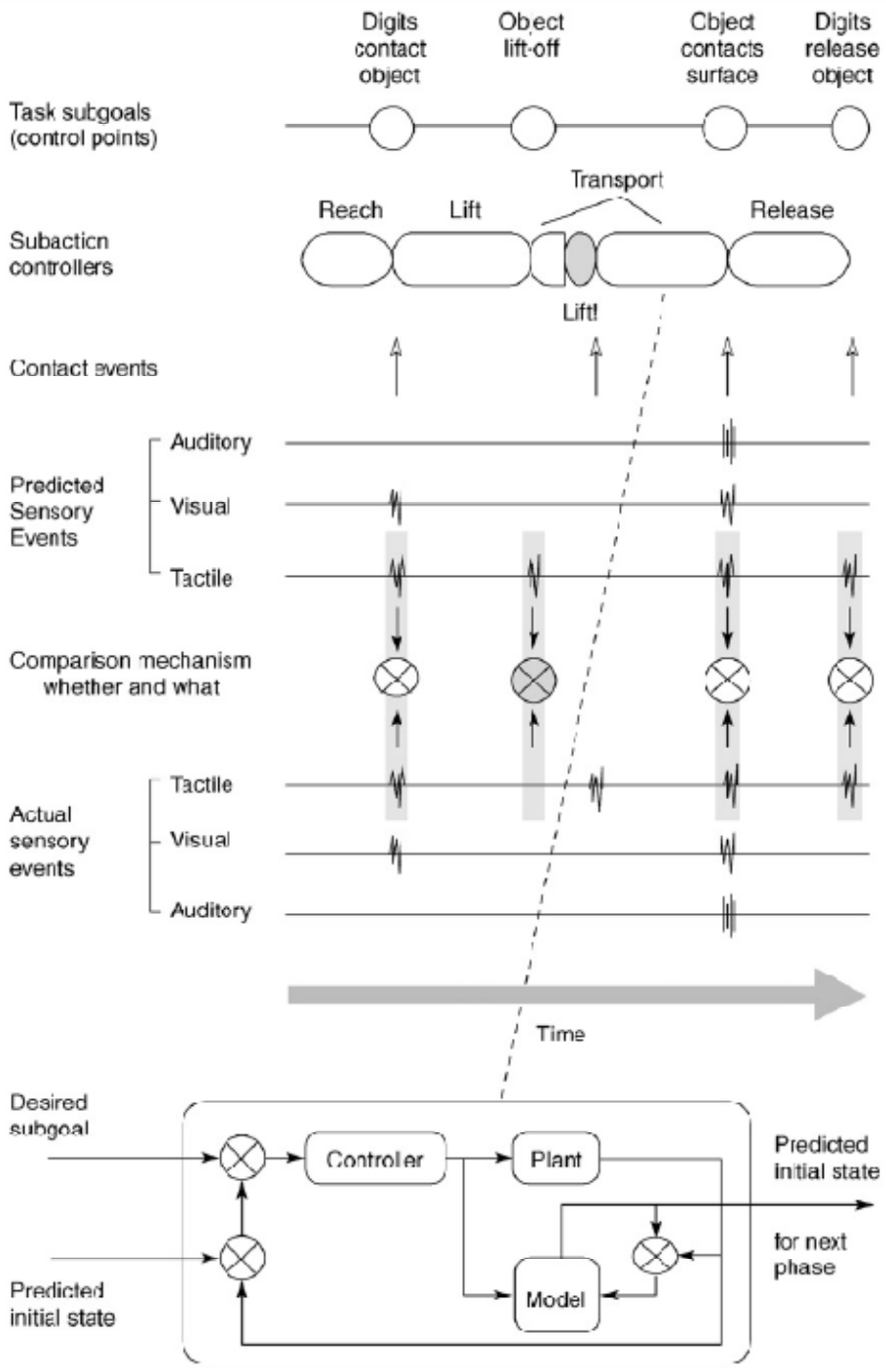

Figure 2.3. Schematic illustration of the phases when human lift up an object [10]

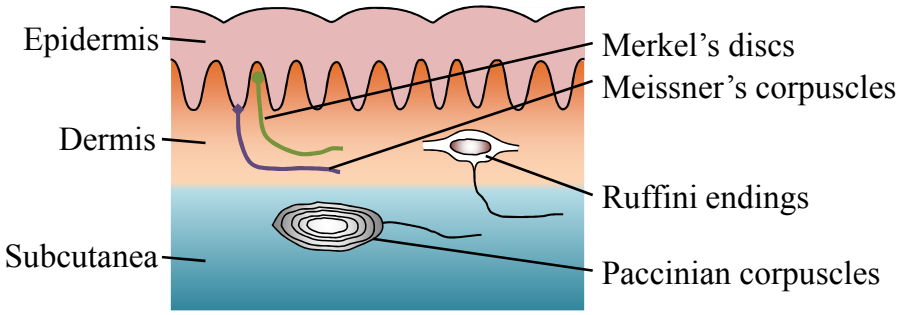

Figure 2.4. Receptors in the skin

developed a tactile sensor with accelerometers which detects minute and high-frequency vibrations at the onset of a partial slip[20]. Tremblay *et al.* developed an improved version of the above sensor[21]. The sensor skin is covered with small "nibs" which vibrate when the incipient slip occurs. This acceleration-based approach is effective for detecting the beginning of the incipient slip; however it seems difficult to measure the degree of the incipient slip since the acceleration measurement is largely affected by noise problem. In order to solve this problem, several tactile sensors have been developed, e.g., based on ultrasonic emission [22] and internal strain distribution sensing [23].

However, these research did not discuss about human like grasp force control. In this thesis, we propose grasp force control method based on human force control strategy using the incipient slip information.

Deep sensation analysis

The deep sensation has two receptors and many endings and corpuscles in the joints and the muscles [24]. Fig. 2.5 shows the sketch of the deep sensation receptors. The influences of these receptors' sensation reach the feeling of the joint angle and the muscle fatigue [25] [26]. However, the human feelings from the deep sensation (almost with the cutaneous sensation) are complex.

The surface EMG (electromyography) is one of the measurable biological signal. The surface EMG is a barometer that indicates human muscle activity. Some research analyzed human grasp using the surface EMG. Inmann *et al.* developed an instrumented object for quantitative evaluation of functional tasks performed

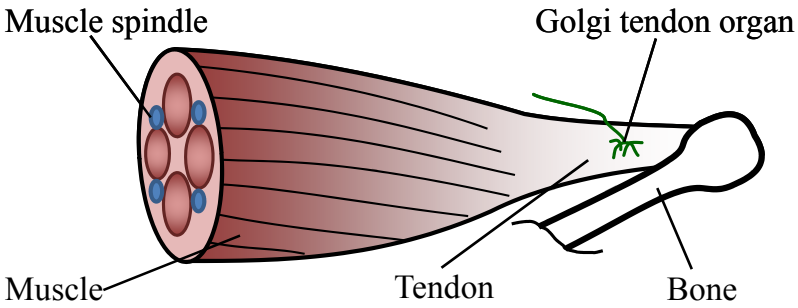

Figure 2.5. Receptors in the muscle and the tendon

with lateral hand grasp [27]. Ogawa *et al.* discussed a quantitative evaluation method of the grip comfort level of electric shavers using a grasp pressure, a trajectory during using the shaver and questionnaire results [28]. Saihara *et al.* discussed the quantitative evaluation of a rechargeable impact driver's usability based on analyzing the body fatigue during using the driver [29]. Amis described an investigation of maximal isometric cylindrical grasping action of the hand [30]. Radhakrishnan *et al.* analyzed the force distribution during tube grasping motions [31]. Kong *et al.* measured the maximum pulling force, the surface EMGs, and the contact force when pulling seven different meat hooks, and developed a biomechanical hand model to estimate the tendon force [32]. They also evaluated the effects of screwdriver handle, surface material and workpiece orientation on torque performance, finger force distribution and muscle activity in a maximum screw driving torque task [33].

These results indicate that the surface EMG can be used for grasp evaluation and the deep sensation is important for human feeling evaluation.

2.3 Human models

Many musculoskeletal models are developed. Fig. 2.6 shows representative whole body models: Nakamura *et al.* [34], *SIMM* (MusculoGraphics. Inc.) [35], *AnyBody* (Cybernet Systems CO. LTD.) [36], *LifeMod* (LifeModeler. Inc.) [37] and *ARMO* (GSport Inc.) [38]. However, the aim of these models is human motion and muscle activity analysis by whole body.

Some research in biomechanics proposed an accurate musculoskeletal model of

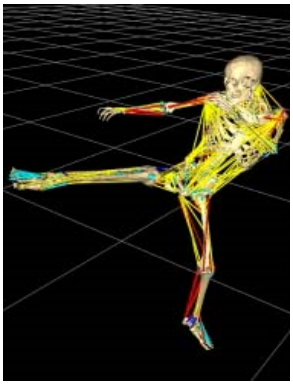

(a) Nakamura's model [34]

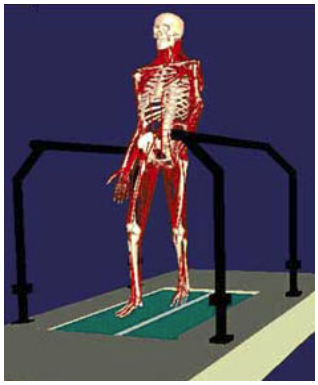

(b) SIMM [35]

(c) AnyBody [36]

(d) LifeMod [37]

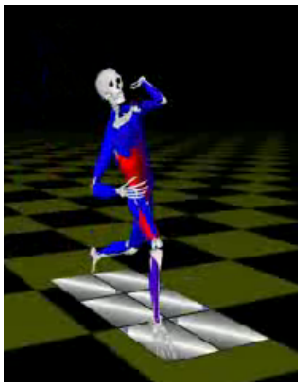

(e) ARMO [38]

Figure 2.6. Human musculoskeletal models

the human hand and fingers. An *et al.* established a three-dimensional normative hand model based on X-ray image analysis [39]. Holzbaur *et al.* developed a model of the upper extremity that includes 15 degrees of freedom representing the shoulder, elbow, forearm, wrist, thumb, and index finger, and 50 muscle compartments crossing these joints [40]. Dennerlein measured the in vivo tendon force of the long finger during passive movement and dynamic tapping of the finger by ten adult patients [41]. Valero-Cuevas proposed a precise model of the human finger, including neuro-musculo-skeletal interactions [42]. Kamper *et al.* showed the importance of muscle moment arms occur with finger posture when constructing biomechanical models of the hand by comparison the human muscle activity with the joint torque [43]. The accuracy of these models were proved in limited situation that like a key pinch.

Some musculo-tendon models are proposed for a realistic CG animation. Tsang *et al.* developed a realistic skeletal musculo-tendon model of the human hand and forearm, and proposed a solution to the inverse problem of determining an optimal set of muscle activations to achieve a given pose or motion [44]. Sueda *et al.* described an automatic technique for generating the motion of tendons and muscles under the skin of an animation character [45]. These models aim to imitating the shape and motion of human muscles and tendons.

On the other hand, a few research proposed human skin and receptor model. Maeno *et al.* calculated in detail the deformation of finger tissue using a FE (finite element) finger model [46] [47] [48]. These studies discussed about the relationship between the finger tissue deformation and the receptors under the skin. Tada *et al.* developed a simple finger shell model that is efficient to quickly simulate the finger surface deformation [49].

However, studies of previous human modeling aim human motion and characteristic analysis. In this thesis, we utilize these knowledge to evaluate grasp effort.

2.4 Summary

This chapter introduced the related work of this thesis. Some research proposed a method of grasp effort evaluation based on the physical restraint. However, many research results of human grasp analysis indicate that the human sensations (the

cutaneous sensation and the deep sensation) are very important for evaluation of humans feeling during grasping an object.

On the other hand, the human musculoskeletal models and skin models were presented. These models can calculate the muscle activity and the skin deformation. However, these studies did not discuss about relationship between the muscle activity and the human sensation.

In this paper, we propose the finger model and the force control method for the grasp effort evaluation using the knowledges of the previous research.

Chapter 3

Human pinching experiment

In this chapter, we discuss about the influence of the muscle force and the tendon force on the grasp effort. Because the muscle force and the tendon force have an influence on the perception of an object weight and own motion.

However, It is difficult to measure the muscle force and the tendon force. The surface EMG is measured instead of the muscle force and the tendon force. We show that the surface EMG reflect the questionnaire result and thus the product usability could be quantitatively estimated from muscle activities.

3.1 Measurement system

Fig. 3.1 shows an overview of the experiment to measure human pinching motion. A capacitance triaxial kinesthetic sensor (PD3-32-05-80, Nitta) was built into the cylinders to measure pinching force. Disposable radiolucent electrodes (F-150S, Nihon Kohden) were put on the hand and the arm of the subject to measure the surface EMG of the FDS (flexor digitorum superficialis) muscle and the ADP (adductor pollicis muscle). The FDS muscle flexes the PIP joint of the index finger, and the ADP muscle adducts the CM joint of the thumb. Fig. 3.2 shows the normal location of muscles in the forearm and the hand. Table 3.1 shows a list of the muscles that drive the index finger and the thumb. In the table, mainly functions of each muscles is described. However, these muscles relate other joint motion because the tendons are constructed complex network.

The surface EMG were amplified by an EMG amplifier (EMG-021, Harada Electronics Industry) and stored in a PC through an A/D board (CSI-360116, Interface).

Fig. 3.3 shows the cylinders used in the experiment. These cylinders are made of ABS (acrylonitrile butadiene styrene) resin. Dimension of the cylinders are 20, 40, 60, 80 and 100 [mm] in length and 20 [mm] in diameter.

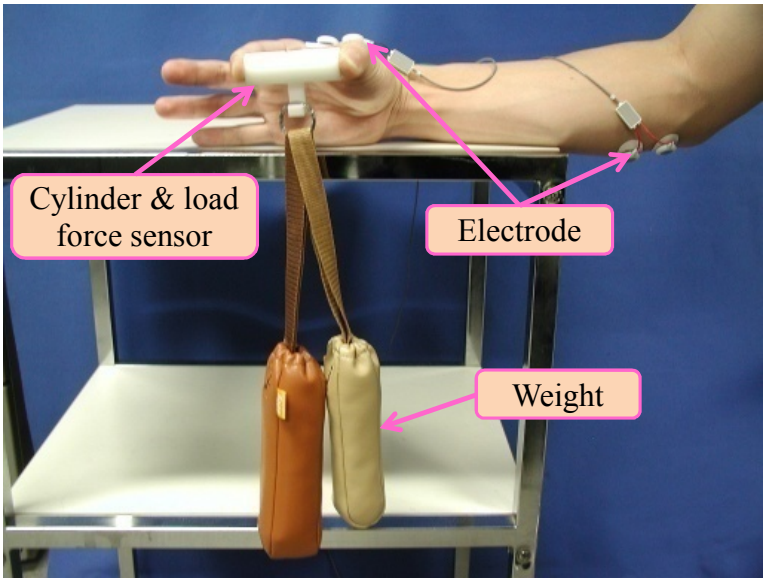

Figure 3.1. Experiment overview of pinching object

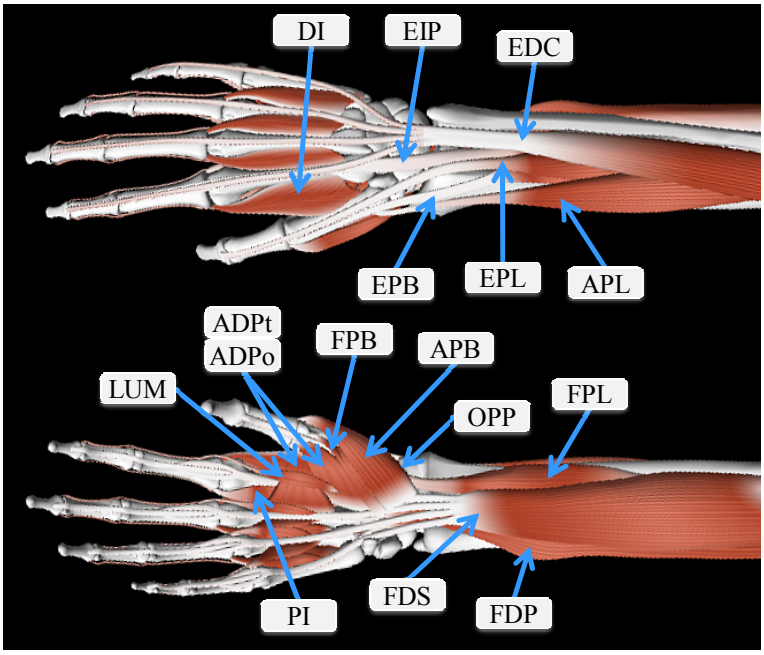

Figure 3.2. Muscles that drive the index finger and the thumb

Table 3.1. List of muscle in the hand and the fore arm

muscle name	main function
Index finger	
flexor digitorum profundus muscle (FDP)	DIP joint flexion
flexor digitorum superficialis muscle (FDS)	PIP joint flexion
extensor indicis proprius muscle (EIP)	MCP joint extension
extensor digitorum proprius muscle (EDC)	MCP joint extension
lumbricalis muscle (LUM)	MCP joint flexion, PIP and DIP joint extension
dorsal interosseous muscle (DI)	MCP joint flexion, PIP and DIP joint extension
palmar interosseous muscle (PI)	MCP joint flexion, PIP and DIP joint extension
Thumb	
flexor pollicis longus muscle (FPL)	IP joint flexion
flexor pollicis brevis muscle (FPB)	MP joint flexion
extensor pollicis longus muscle (EPL)	IP joint extension
extensor pollicis brevis muscle (EPB)	MP joint extension
abductor pollicis longus muscle (APL)	CMC joint extension and abduction
abductor pollicis brevis muscle (APB)	CMC joint abduction
the transverse head of the adductor pollicis muscle (ADPt)	MP joint flexion
the oblique head of the adductor pollicis muscle (ADPo)	MP joint flexion
opponents pollicis muscle (OPP)	CMC joint abduction

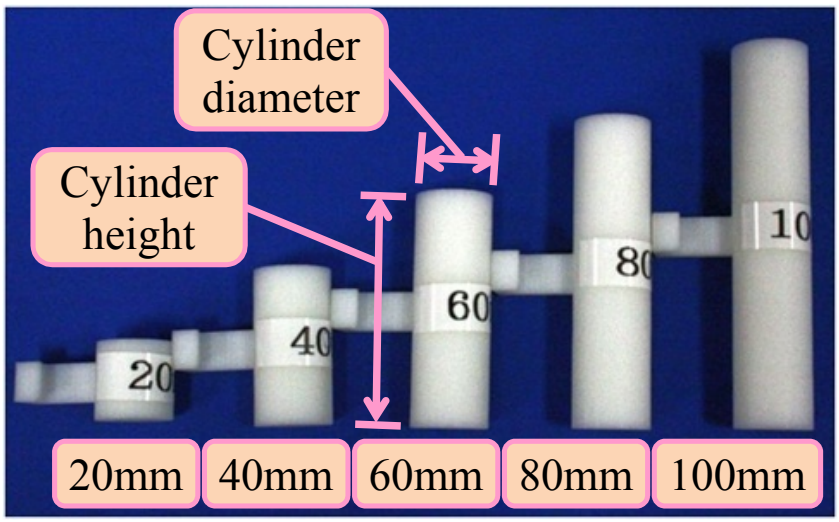

Figure 3.3. Cylinder dimensions

3.2 Experimental method

In our experiment, 300 [g] and 600 [g] weights are used. Five healthy male subjects, aged 22 to 30 years old, volunteered for the experiment. All subjects were given the experimental detail and they gave their consent to participate. The pinching motion was conducted by their dominant arm. The arm of the subject was placed on a desk, and the middle, ring, and little fingers were kept open so as not to influence the pinching motion. Subjects pinch in the length direction of the cylinder by using the index finger and thumb. Table 3.2 shows the average and standard deviation of the subjects' hand sizes. Fig. 3.4 shows the measured parts of the hand. The subjects' hand sizes were similar to the standard Japanese hand size.

Before beginning the experiment, we explained its purpose to the subjects. In the experiment, the subjects pinched each cylinder and scored the effort level of the cylinder. The score had five levels from 1: "very easy to pinch" to 5: "very difficult to pinch". The subjects pinch a cylinder in arbitrary order. A two-minute interval was taken between each trial.

Then, the subject joint angle when pinching each cylinder was measured by the CyberGlobe (CyberGlove Systems LLC). Fig. 3.4 shows the joint name of the index finger and the thumb. We measure the eight angles: the MCP

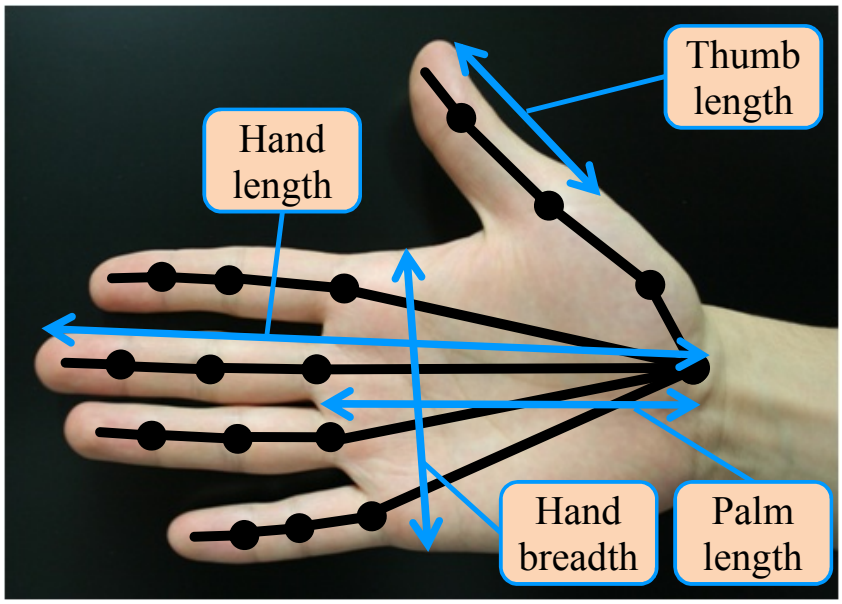

Figure 3.4. Measured dimensions

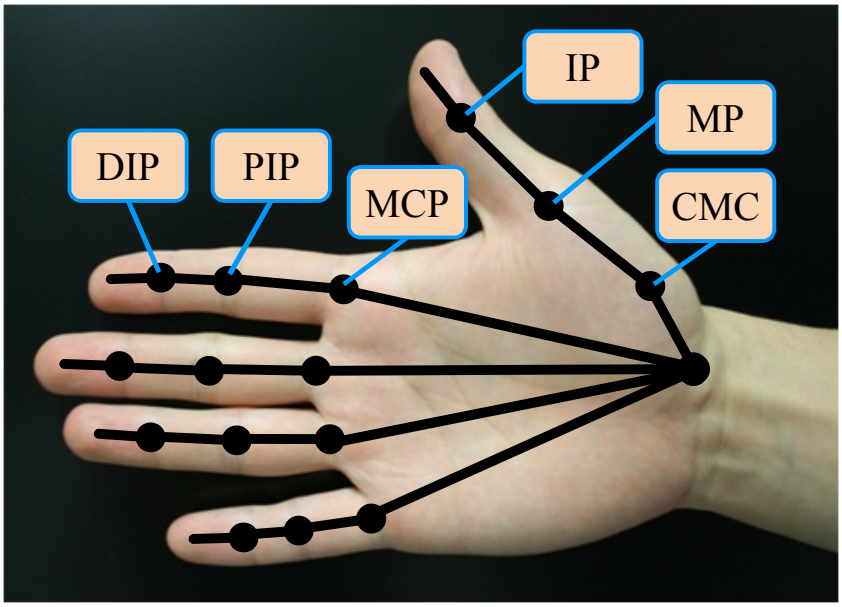

Figure 3.5. Joint name of the index finger and the thumb

(metacarpophalangeal: in the index finger) joint FE (flexion/extension direction), the MCP joint AA (adduction/abduction direction), the PIP (proximal interphalangeal) joint FE, the DIP (distal interphalangeal) joint FE, the CMC (carpometacarpal) joint FE, the CMC joint AA and the MP (metacarpophalangeal: in the thumb) joint FE. We can not measure the MP joint AA and the IP (Interphalangeal) joint FE because there are not sensors in the CyberGlobe. The human joint angles are compared with simulation results in capter 5.

3.3 Human experimental results

3.3.1 Questionnaire survey results

Fig. 3.6 shows the average and standard deviation of the scores. The curves in the figure are the approximate quadratic curves of the 300 [g] and 600 [g] weights. The lowest score is observed in the 60 [mm] cylinder length for both the 300 [g] and 600 [g] weights. On the other hand, the higher score is observed when the cylinder length is 20 and 100 [mm] for both the 300 [g] and 600 [g] weights. The possible reason is that the finger posture when pinching the middle length cylinder makes it easy to exert pinching force.

3.3.2 Pinching force measurement results

Fig. 3.7 shows the typical pinching force when subject pinches a cylinder. The dash line and the dot-dash line in the figure mean the theoretically necessary force to pinch the cylinders with 300 [g] and 600 [g] weight, respectively. The theoretically necessary forces F_{theo} are calculated based on the friction coefficient

Table 3.2. Average and standard deviation of hand size

	Ave.	SD
Hand length [mm]	184.4	5.5
Palm length [mm]	104.6	4.7
Hand breadth [mm]	82.6	5.3
Thumb length [mm]	61.6	2.8

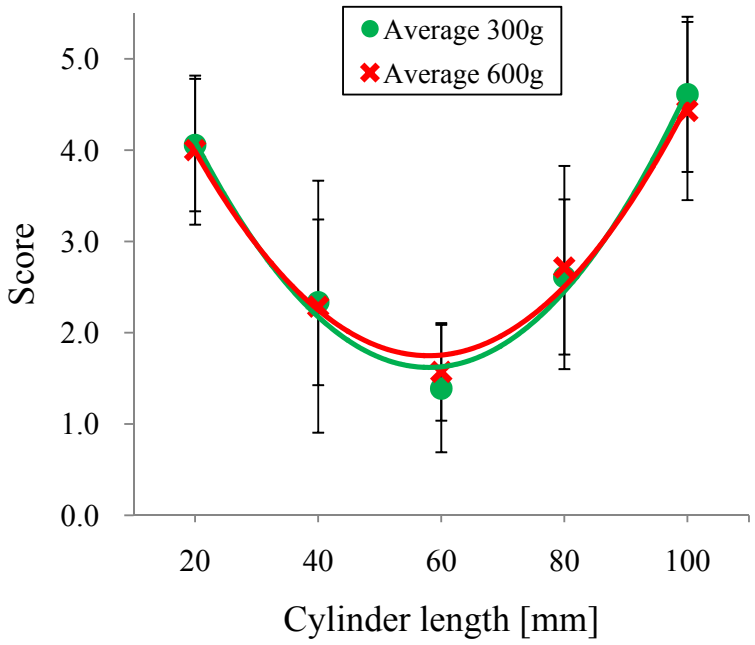

Figure 3.6. Questionnaire results

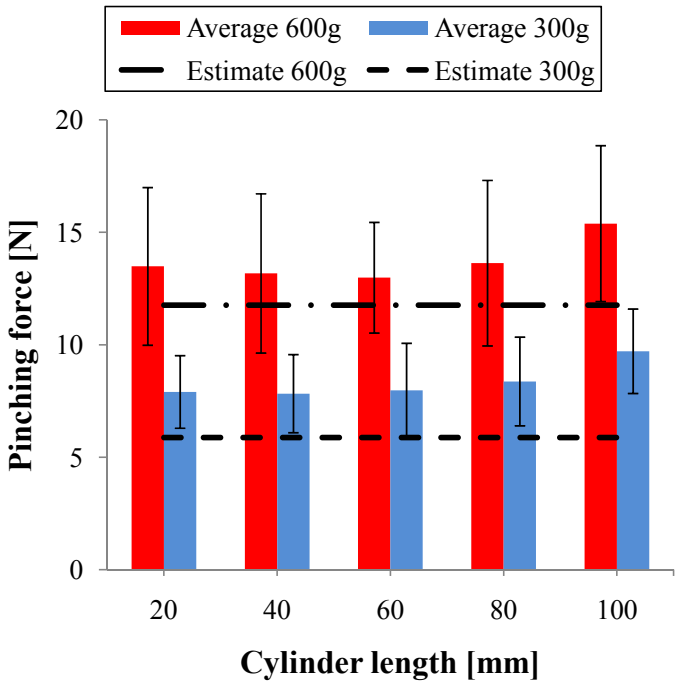

Figure 3.7. Pinching force

μ between the finger and the cylinder:

$$F_{theo} = \mu M_{obj} \tag{3.1}$$

where M_{obj} is a weight of the object and $\mu = 0.5$. The measured pinching force is larger than the theoretically necessary force because a human applies a safety margin in order to grasp an object tightly.

The highest pinching force is observed when a subject pinches the 100 [mm] cylinder for both weights. The possible reason is that the 100 [mm] is hardest to pinch.

3.3.3 Surface EMG measurement results

We evaluate pinching effort from the integrated surface EMG during the pinching motion. The integrated surface EMG were normalized using the minimum and maximum values of the integrated surface EMG during the experiment.

Fig. 3.8 shows the normalized EMG related to the index finger and thumb when the cylinder weight is 300 [g], and Fig. 3.9 shows the normalized EMG when the cylinder weight is 600 [g]. The normalized EMG of the index finger FDS becomes lower according to the cylinder length, and the normalized EMG of the thumb ADPt becomes higher according to the cylinder length. The possible reason is that the finger posture when pinching a short cylinder makes it hard for the index finger to exert pinching force. On the other hand, when pinching a long cylinder, a large antagonist force is necessary to open the thumb widely, and thus the muscle activity of the thumb increases.

Fig. 3.10 shows the average EMG and the questionnaire score when the cylinder weight is 300 [g], and Fig. 3.11 shows the average EMG and the questionnaire score when the cylinder weight is 600 [g]. The lowest score is observed when human pinches the cylinder with the lowest EMG, and the highest score is observed when human pinches the cylinder with the highest EMG. The correlation coefficients between the average EMG and the questionnaire result are 0.86 at 300 [g] and 0.97 at 600 [g]. The p-values are 0.061 at 300 [g] and 0.005 at 600 [g]. There are correlations between the surface EMG and the questionnaire result, but the p-value of 300 [g] result is high ($p > 0.05$). The possible reason is that the 300 [g] weight was too light to evaluate the grasp effort. These results mean that

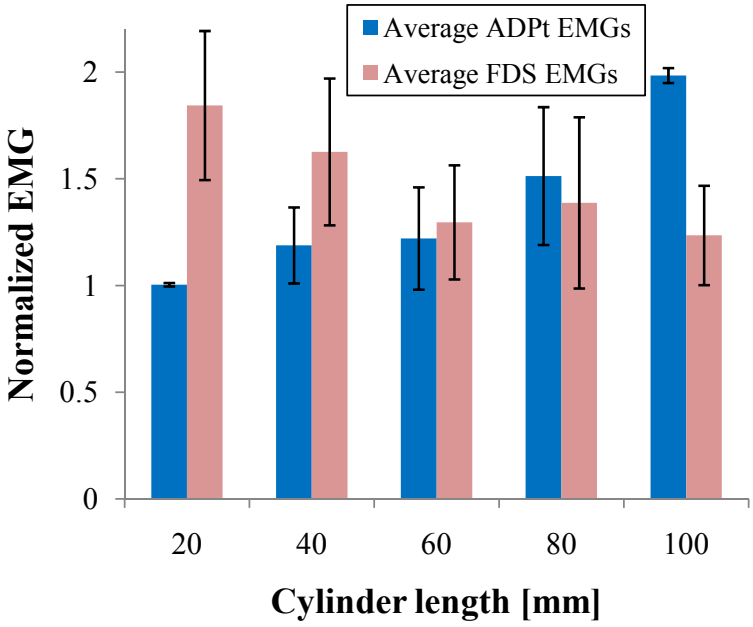

Figure 3.8. Integrated EMG (300[g])

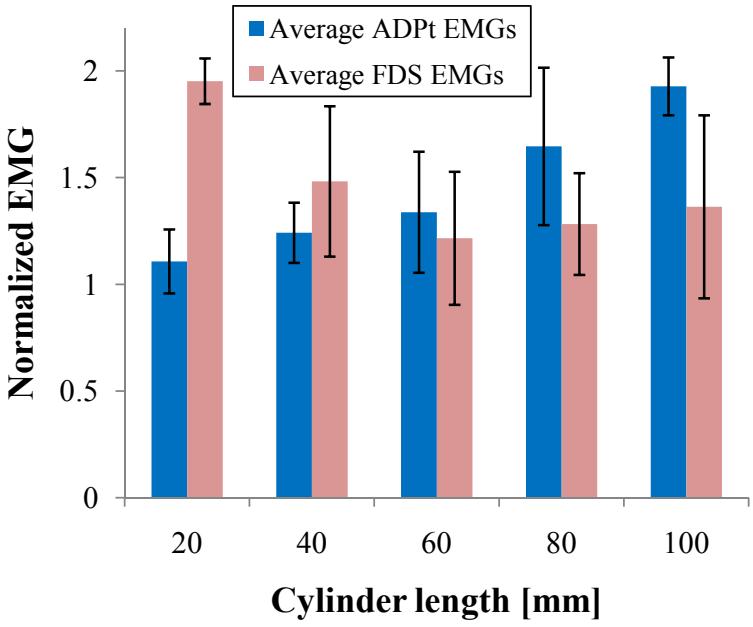

Figure 3.9. Integrated EMG (600[g])

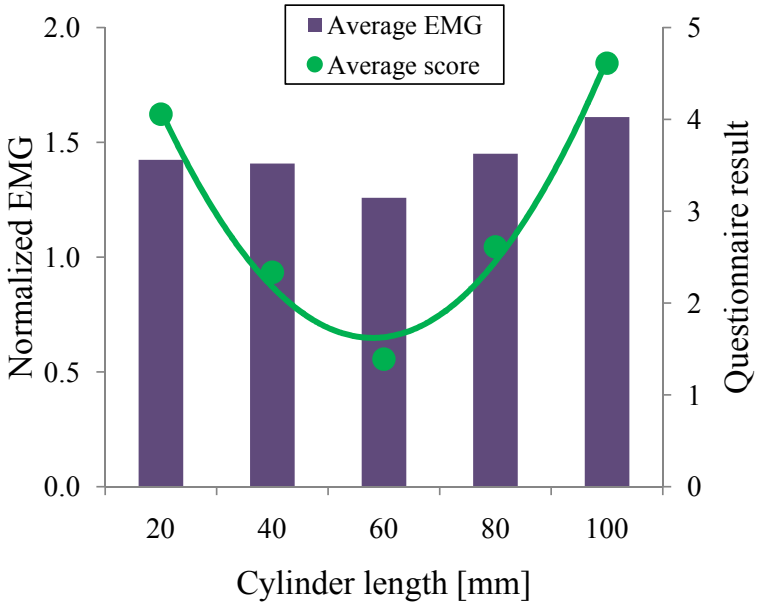

Figure 3.10. Average EMG and questionnaire score (300[g])

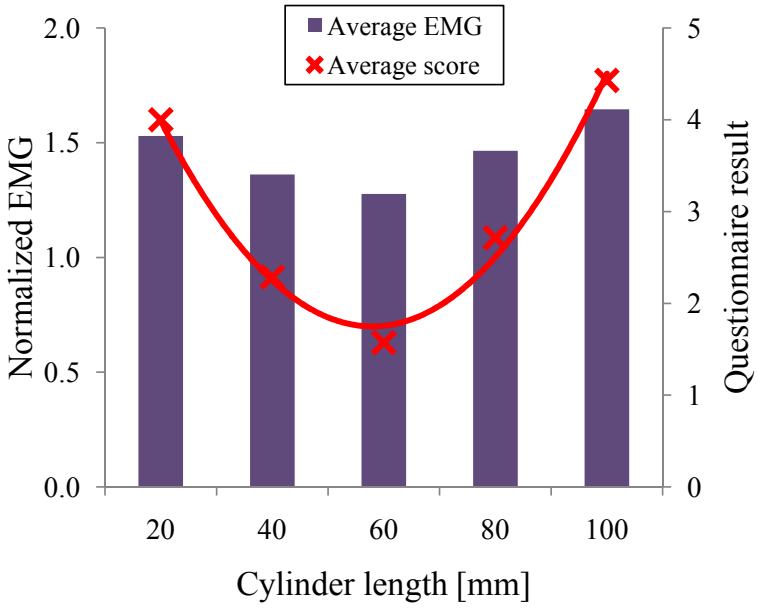

Figure 3.11. Average EMG and questionnaire score (600[g])

the integrated surface EMG is one of the important indexes to indicate grasp effort. These results indicate a possibility that the quantitative evaluation using the muscle or tendon force.

3.4 Summary

This chapter showed the experimental results when human pinches the cylinder. We measured the subjective pinching effort, the pinching force, the surface EMG and the finger posture duging pinching motion. We found that the surface EMG has important correlation with the human pinching effort. These results indicate a possibility that the quantitative evaluation using the muscle or tendon force.

Chapter 4

Grasp effort score calculation method

In this chapter, we explain the calculation method of the grasp effort score using the tendon force margin. The tendon force margin of each tendon is calculated from a load in tendons which is connected to each muscle and a maximum force of each muscle. It means that the tendon force margin is a barometer of human muscle force. At first, the calculation flow of the grasp effort score is shown. The score is calculated from the grasp force using the tendon skeletal model of the index finger and the thumb. Next, the vision based grasp force control method is explained. This force control method is based on the incipient slip information of the fingertip. Then the tendon skeletal model and the finger posture estimation method are explained. The tendon skeletal model is constructed based on human moment arm data.

4.1 Tendon force margin estimation

The grasp effort score is defined by following equation:

$$Score(F_{tendon}) = \frac{1}{n}\sum_{i=1}^{n}\frac{f_i}{f_{imax}} \rightarrow \min \tag{4.1}$$

where n is a number of the tendon used for grasp an object. For example, when only the index finger used, n is 7, and when the index finger and the thumb used, n is 16. f_i is the tendon force of each tendon and f_{imax} is the max force that the muscle can exert to each tendon. We call f_i/f_{imax} the tendon force margin. It means the load ratio of each tendon. So, the minimum score means a condition of minimum load for human.

Fig. 4.1 shows the calculation flow of the score. The proposed method has following steps:

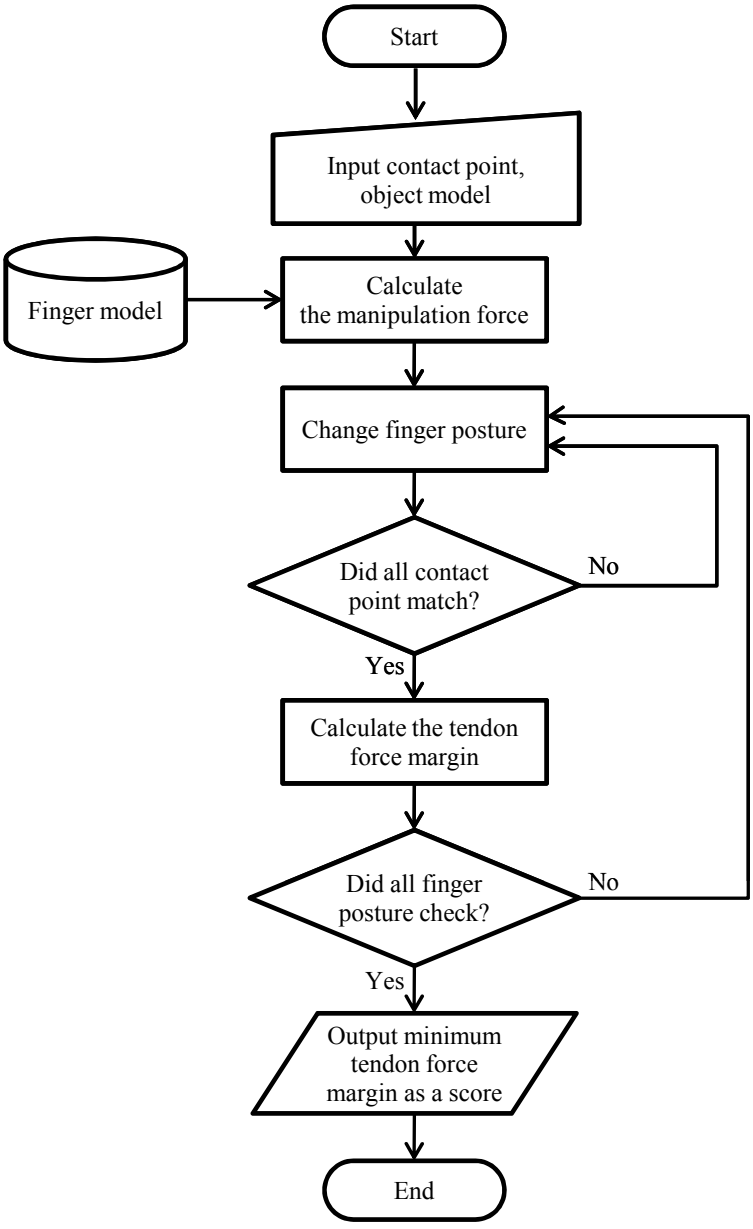

Figure 4.1. Calculation flow

Step 1:

Operator input an object model and the contact points to grasp the object. The object model includes its weight, center of mass and friction of surface.

Step 2:

A system load the finger model from a database.

Step 3:

The grasp force is calculated from the object weight and the friction of surface using the vision based grasp force control method.

Step 4:

The finger joint angle is changed independently.

Step 5:

The finger posture that the finger tips match to the contact points is searched. Step 4 and 5 are repeated while not matching the finger tips to the contact points.

Step 6:

The tendon force margin is calculated using the grasp force and the finger posture. The tendon force margin is stored to the end of this flow. Step 4 to 6 are repeated while the joint angles in the range of motion.

Step 7:

The minimum value of stored tendon force margin is decided as a grasp effort score. The finger posture of the minimum tendon force margin is determined as a human like grasp posture.

4.2 Grasp force control

4.2.1 Contact between an elastic object and a rigid plate

The contact between an elastic sphere and a rigid plate is called *Hertzian contact* [50] and various analysis have been presented [51]. Fig. 4.2 shows the schematic diagram of the contact when applying a normal (grasp) force f_g and a tangential (traction) force f_l. In this analysis, we consider the situation where the contact

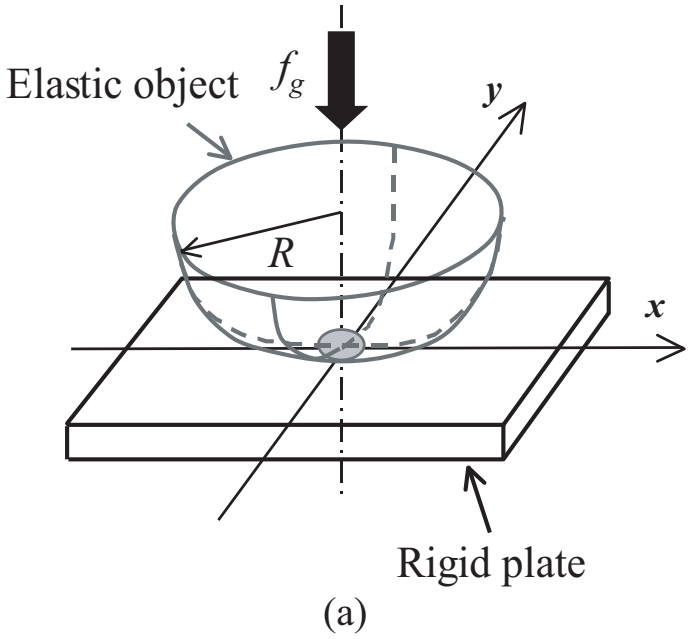

(a) Applying a normal force

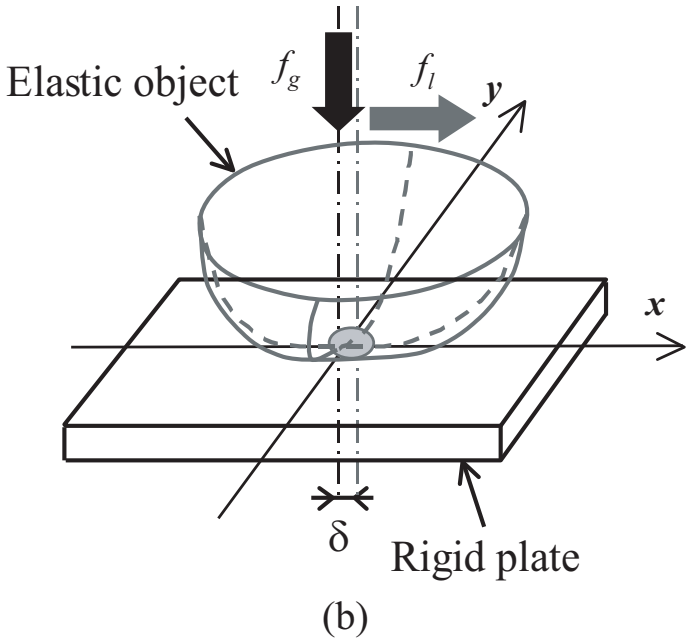

(b) Applying a normal and tangential force

Figure 4.2. Contact model of an elastic object and a rigid plate

holds, therefore $f_g > 0$. Considering the sphere is symmetric around the direction of f_g, we can assume that f_l denotes the absolute value of the tangential force without losing the generality, i.e., $f_l > 0$.

When the elastic sphere is pressed and slid on a rigid plate, the sphere deforms depending on f_g and f_l. The radius of the contact area a is derived from the following equation:

$$a = \left(\frac{3 f_g R}{2E'} \right)^{1/3} \tag{4.2}$$

where R is the radius of the elastic object and $E' = 2/\{(1-\nu_1^2)/E_1 + (1-\nu_2^2)/E_2\}$ is the equivalent stiffness coefficient. Young's modulus and Poisson's ratio of the elastic object and the rigid plate are E_1, ν_1 and E_2, ν_2, respectively.

The distribution of the normal pressure $P(f_g, r)$ in the contact area and the maximum normal pressure $P_{max}(f_g)$ are derived from the following equation [50]:

$$P(f_g, r) = \frac{3 f_g}{2\pi a^2} \left(1 - \frac{r^2}{a^2} \right)^{1/2} \tag{4.3}$$

where $r = \sqrt{x^2 + y^2}$ and $[x, y]$ is the position based on the contact center. The maximum normal pressure is given by: $P_{max} = 3 f_g / (2\pi a^2)$. The normal force around the boundary is smaller than the normal force around the center. Therefore a slip between the elastic object and the rigid plate occurs from the boundary region.

When the whole contact surface slips, the elastic object begins to slip completely to the rigid plate, which is called the "gross slip". The partial slip that occurs before the gross slip is called the "incipient slip" [17]. In this paper, the contact region where a partial slip occurs is called as the slip region. The contact region where the objects surface is stuck is called as the stick region. The distance c from the contact center to the boundary between the stick region and the slip region is given by[50]:

$$c = a(1 - \Phi)^{1/3} \tag{4.4}$$

where $\Phi \triangleq f_l/\mu f_g$ is the tangential force coefficient. μ is the friction coefficient of the contact area. The distribution of the tangential pressure $T(f_g, r)$ in the slip region and the stick region are derived as follows [50]:

$$T(f_g, r) = \begin{cases} \mu P_{max} \left(1 - \frac{r^2}{a^2}\right)^{1/2} \\ \qquad \text{(Slip region : } c < r \leq a\text{)} \\ \mu P_{max} \left(1 - \frac{r^2}{a^2}\right)^{1/2} \left(1 - \frac{c}{a}\right) \\ \qquad \text{(Stick region : } 0 < r \leq c\text{)} \end{cases} \tag{4.5}$$

The tangential pressure becomes maximum on the boundary between the stick region and the slip region. Suppose the elastic object deforms by applying f_g and f_l. A relative displacement δ as shown in Fig. 4.2(b) is occurred by the deformation of the elastic object. The analytic solution is given by the following equation[51]:

$$\delta = \frac{3\mu f_g}{16a} \left(\frac{2-\nu}{G}\right) \left\{1 - (1 - \Phi)^{2/3}\right\} \tag{4.6}$$

where $G = E/\{2(1+\nu)\}$. Note that the equation (4.6) holds when both bodies in contact are linear elastic and the deformation is small. Hence, nonlinear behavior, e.g., a very large deformation, is not considered. From these assumptions, the contact area is assumed circular. Recently, Xydas *et al.* presented that the radius of contact is proportional to the normal force raised to the power of from 0 to 1/3[52]. In this sense, the Hertzian contact model in (4.2) is only a part of this model. However, this model has not been expanded to the case where the normal and the tangential force are simultaneously applied. In this paper, an analytic solution of the deformation of the elastic object is required for this case. Therefore, the analytic result based on the *classic* Hertzian model in (4.6) is applied.

4.2.2 Slip margin

In order to keep the contact without slip, the normal force f_g corresponding to the traction force f_l should be determined so as to satisfy the friction condition

given by the friction cone. The slip margin $\gamma(0 \leq \gamma \leq 1)$ is used as an index of this contact stability:

$$\gamma = 1 - \Phi \tag{4.7}$$

When the contact area is completely stuck, $\gamma = 1$ holds. The incipient slip occurs as γ decreases and the elastic object completely slips when $\gamma = 0$. As shown in (4.7), the slip margin γ is easily obtained if Φ is given. It can be said that the estimation of Φ is almost equivalent to the estimation of γ. Hereafter, we use "slip margin" to refer to Φ unless it causes a confusion.

4.2.3 Vision-based control of grasp force

Fig. 4.3 shows the result of a preliminary experiment. The contact area is measured by a camera through a transparent plate. A feature point(dot) is drawn on the apex of an elastic sphere. In the figure, the bright area presents the contact area, and the feature point is showed by the intersection of two orthogonal lines. When the traction force is increased, the object begins to slip from the boundary of the contact area and the slip region expands toward the center. Therefore, the relative position of the feature point, which is in the stick region in the contact area, changes whose displacement is given by (4.6).

As described above, there exist slip region and stick region in the contact area. The diameter of the stick region becomes small according to (4.4) by increasing the traction force; however, this change of the stick region can not be directly observed by a camera.

The basic concept of this paper is to estimate the slip margin, i.e., the change of the stick region, based on the displacement of the feature point. The estimated slip margin is used to calculate the grasp force as shown in Fig. 4.4. By estimating the margin during the incipient slip, a stable grasping is realized against the change of the traction, e.g., disturbance force.

4.2.4 Grasp force control based on estimated slip margin

In this section, a method of estimating Φ is presented by applying (4.6). In (4.6), G and ν are known material constants of the elastic object. Then, δ, μ, f_g, and

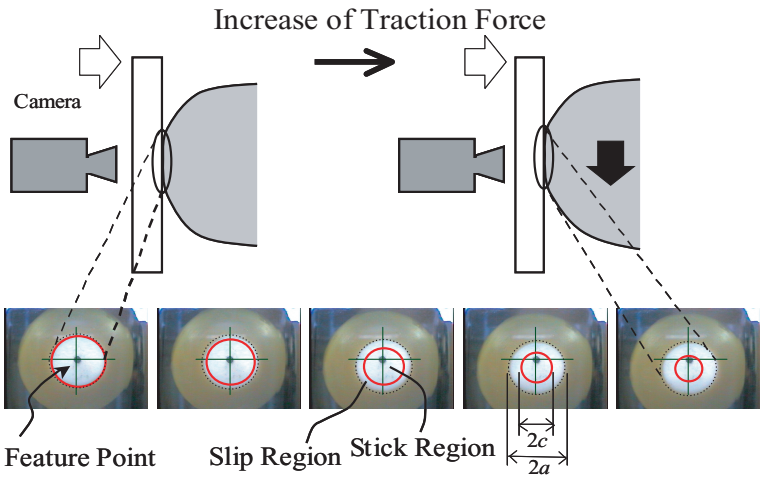

Figure 4.3. Deformation of the Contact Area

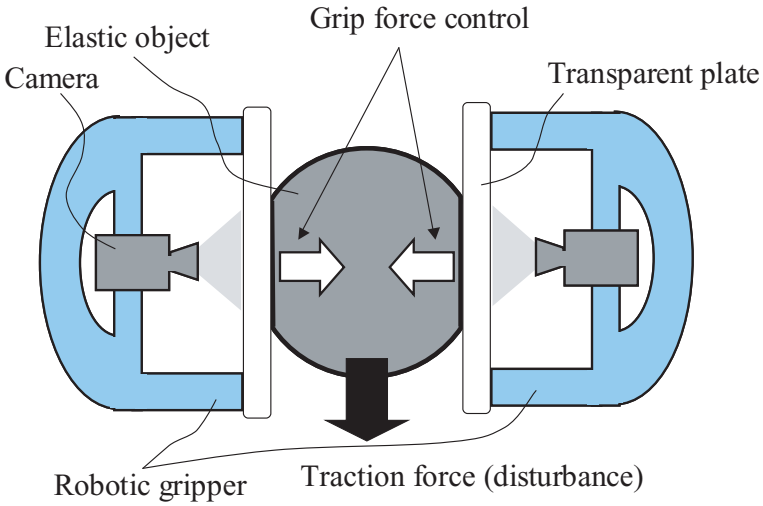

Figure 4.4. Concept of Vision-based grasp Control

a are needed to estimate Φ by inverse solution of (4.6). As will be shown in the following sections, we use a camera to measure the contact surface, then δ and a are measured from this image. Additionally, f_g is obvious since it is the output of the actuator itself. The remaining unknown variable is the friction coefficient μ; however we focus on the grasp-force control without knowing μ, therefore the following transformation of (4.6) is applied dividing both sides by f_l.

$$\frac{\delta}{f_l} = \frac{3}{16a}\frac{1}{\Phi}\left(\frac{2-\nu}{G}\right)\left\{1-(1-\Phi)^{2/3}\right\} \tag{4.8}$$

The following equation is obtained by collecting Φ:

$$\alpha^3\Phi^2 + (1-3\alpha^2)\Phi + (3\alpha - 2) = 0 \tag{4.9}$$

where $\alpha = 16Ga\delta/(6-3\nu)f_l$.

The solution of (4.9) Φ_1 and Φ_2 are obtained as follows:

$$\Phi_1 = \frac{-(1-3\alpha^2) - \{(1-3\alpha^2)^2 - 4\alpha^3(3\alpha-2)\}^{1/2}}{2\alpha^3} \tag{4.10}$$

$$\Phi_2 = \frac{-(1-3\alpha^2) + \{(1-3\alpha^2)^2 - 4\alpha^3(3\alpha-2)\}^{1/2}}{2\alpha^3} \tag{4.11}$$

Fig. 4.5 shows an example of the plot obtained by two solutions Φ_1 and Φ_2. In calculation of Fig. 4.5, $f_l = 10.0$[N], $\mu = 0.5$ are used. As can be seen in above derivation, the estimation becomes impossible when $f_l = 0$. Therefore, the condition $f_l = 0$ was avoided for the calculation. Since the admissible traction force $\tilde{f_l}$ is given by $\tilde{f_l} = \mu f_g = 5$[N], a partial (incipient) slip occurs in the range where $0 < f_l < 5$, then the gross slip occurs where $f_l \geq 5$. Recall $\Phi = f_l/\mu f_g$, then it is clear that Φ_1 corresponds to Φ in the incipient slip condition. In contrast, Φ_2 corresponds to Φ in the gross slip condition.

Based on these analyses, Φ_1 in the incipient slip condition can be calculated from (4.10) by measuring δ, f_l, and a. By using this estimated Φ_1, a grasp-force control during the incipient slip can be applied, i.e., it is unnecessary to estimate μ by slipping the object once in the gross slip condition.

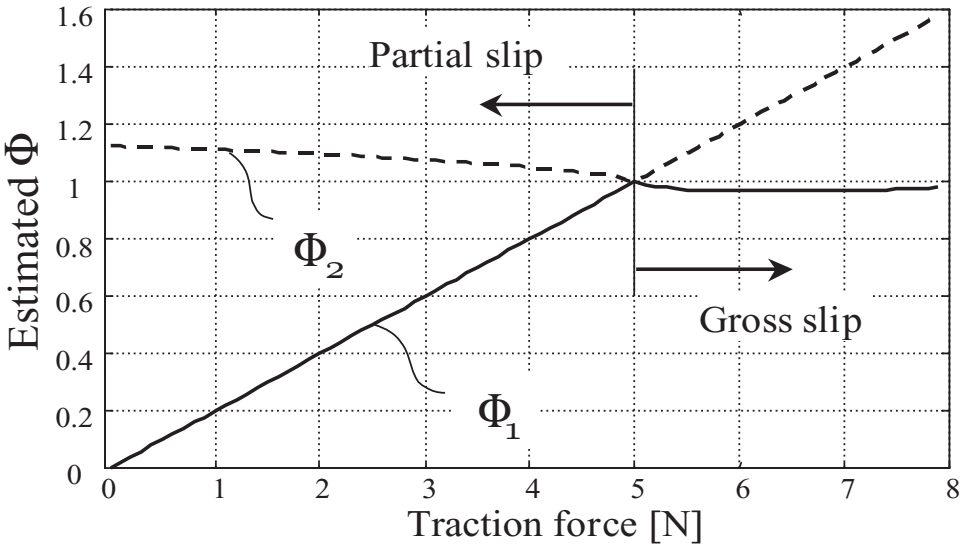

Figure 4.5. Estimation of Φ

The grasp force is controlled by a direct and linear feedback of the slip margin:

$$\begin{aligned} \dot{f}_g &= k(\gamma_d - \gamma(t)) \\ &= k(\Phi(t) - \Phi_d) \end{aligned} \tag{4.12}$$

where $k(>0)$ is a feedback gain and $\gamma_d = 1 - \Phi_d$ is the target slip margin.

4.3 Finger model

4.3.1 Tendon skeletal model

Fig. 4.6 and Fig. 4.7 show the index finger model and the thumb finger model. The index finger model consists of a fixed metacarpal and three phalanges. The DIP and the PIP joints have 1 DOF (degree of freedom) for flexion/extension, and the MP joint has 2 DOF for flexion/extension and adduction/abduction. The thumb model contains a fixed trapezium bone and three phalanges. The IP joint has 1 DOF for flexion/extension, and the MP and the CM joints have 2 DOF for flexion/extension and adduction/abduction.

It is difficult to construct an anatomically accurate finger model because the human hand structure is very complex. Some research discussed the importance

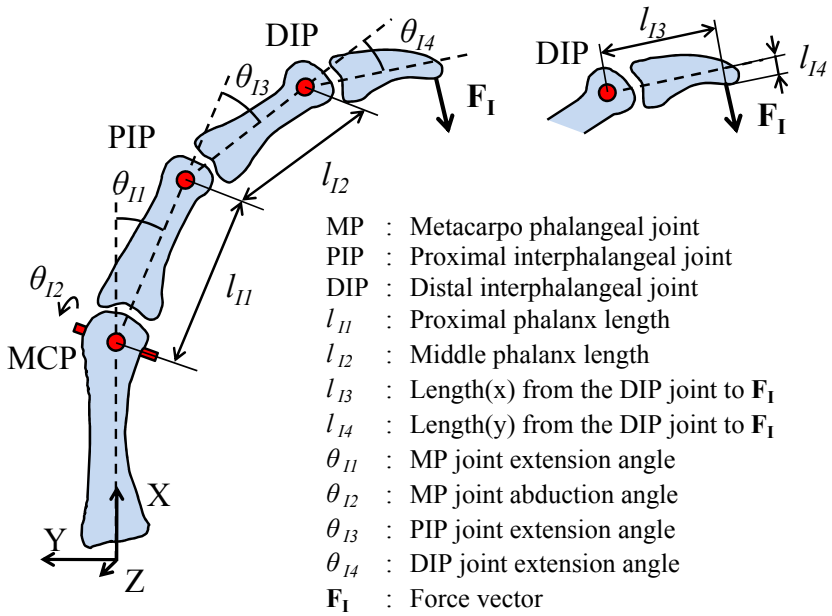

Figure 4.6. Index finger model

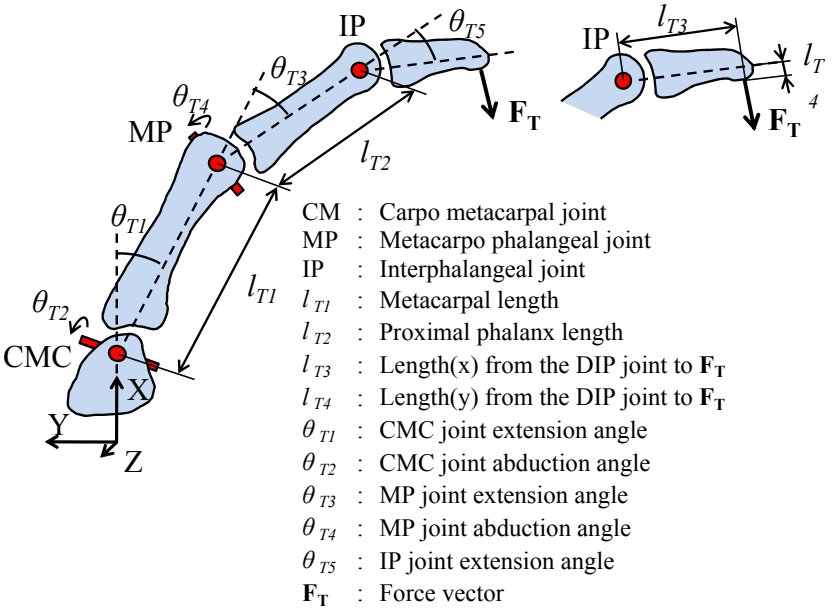

Figure 4.7. Thumb finger model

between the finger posture and the moment arm when exerting the fingertip force [53] [54]. Kamper *et al.* discussed importance of finger posture and moment arm when mapping from muscle activation to joint torque [43]. The index finger joint torques $\boldsymbol{\tau}_I$ and the thumb joint torques $\boldsymbol{\tau}_T$ were calculated from the following equations:

$$\boldsymbol{\tau}_I = \mathbf{M_I F_{tendonI}} \tag{4.13}$$

$$\boldsymbol{\tau}_T = \mathbf{M_T F_{tendonT}} \tag{4.14}$$

where $\boldsymbol{\tau}_I = \left\{ \begin{array}{cccc} \tau_{DIP} & \tau_{PIP} & \tau_{MCPa} & \tau_{MCPf} \end{array} \right\}^T$ is the vector of the index finger joint torques, $\mathbf{M_I}$ is the matrix of the index finger moment arms at each joint, $\mathbf{F_{tendonI}} = \left\{ \begin{array}{cccccc} f_{FDP} & f_{FDS} & f_{EIP} & f_{EDC} & f_{LUM} & f_{DI} & f_{PI} \end{array} \right\}^T$ is the vector of the index finger tendon forces, $\boldsymbol{\tau}_T = \left\{ \begin{array}{ccccc} \tau_{IP} & \tau_{MPa} & \tau_{MPf} & \tau_{CMCa} & \tau_{CMCf} \end{array} \right\}^T$ is the vector of the thumb joint torques, $\mathbf{M_T}$ is the vector of the thumb moment arms at each joint, and $\mathbf{F_{tendonT}} = \left\{ \begin{array}{cccccccc} f_{FPL} & f_{FPB} & f_{EPL} & f_{EPB} & f_{APL} & f_{APB} & f_{ADPt} & f_{ADPo} & f_{OPP} \end{array} \right\}^T$ is the vector of the thumb tendon forces.

4.3.2 Tendon moment arm

It is well known that the moment arm of each joint changes according to the joint angle. In this thesis, the moment arms $\mathbf{M_I}$ and $\mathbf{M_T}$ are calculated by the quartic approximation which are showed in Fig.4.8 and Fig.4.9. These profiles are given by the quartic approximation based on the row cadavers data that were measured by An *et al.* and Smutz *et al.* [55][56]. The parameters of these approximation are shown in appendix C. The tendon forces are calculated accurately using the variable moment arms.

4.3.3 Tendon force estimation

The joint torques $\boldsymbol{\tau}_I$ and $\boldsymbol{\tau}_T$ can be calculated by using Jacobian matrices:

$$\boldsymbol{\tau}_I = \mathbf{J_I^T F_I} \tag{4.15}$$

$$\boldsymbol{\tau}_T = \mathbf{J_T^T F_T} \tag{4.16}$$

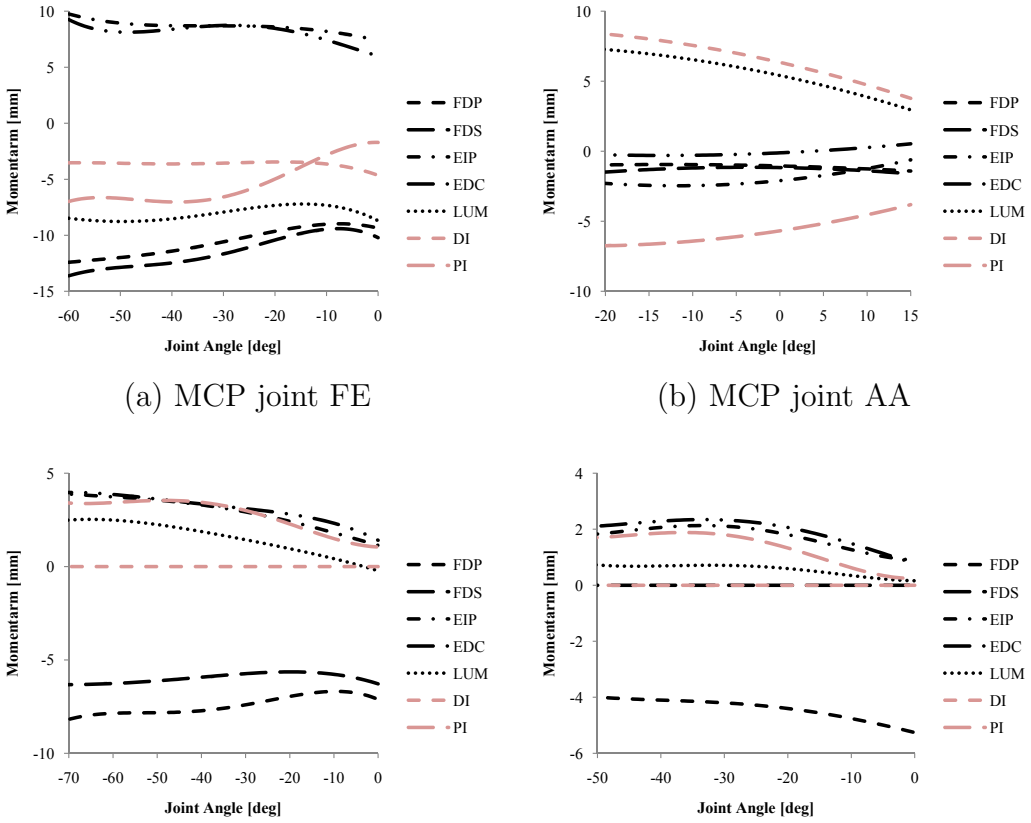

(a) MCP joint FE

(b) MCP joint AA

(c) PIP joint FE

(d) DIP joint FE

Figure 4.8. Index finger moment arms

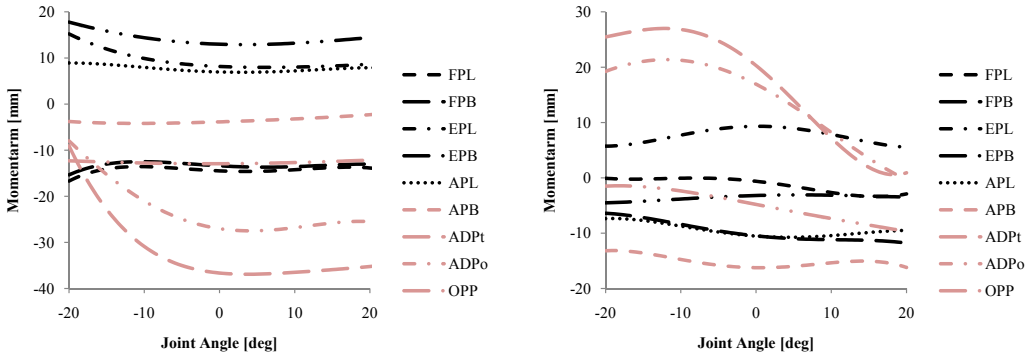

(a) CMC joint FE

(b) CMC joint AA

(c) MP joint FE

(d) MP joint AA

(e) IP joint FE

Figure 4.9. Thumb moment arms

where $\mathbf{J_I}$ is the index finger Jacobian matrix, $\mathbf{J_T}$ is the thumb Jacobian matrix, $\mathbf{F_I} = \left\{ \begin{array}{cccccc} f_{Ix} & f_{Iy} & f_{Iz} & \tau_{Ix} & \tau_{Iy} & \tau_{Iz} \end{array} \right\}^T$ is the index fingertip force and torques, and $\mathbf{F_T} = \left\{ \begin{array}{cccccc} f_{Tx} & f_{Ty} & f_{Tz} & \tau_{Tx} & \tau_{Ty} & \tau_{Tz} \end{array} \right\}^T$ is the thumb fingertip force and torques. The following equations were obtained by substituting Eq. 4.13 to Eq. 4.16:

$$\mathbf{F_I} = \left(\mathbf{J_I J_I^T}\right)^{-1} \mathbf{J_I M_I F_{tendonI}} \tag{4.17}$$

$$\mathbf{F_T} = \left(\mathbf{J_T J_T^T}\right)^{-1} \mathbf{J_T M_T F_{tendonT}}. \tag{4.18}$$

The tendon forces can be calculated from the fingertip forces based on Eq. 4.17 and Eq. 4.18. However, it is a redundant problem because 6 DOFs of the finger are driven by 7 tendons for the index finger, and 6 DOFs are driven by 9 tendons for the thumb. Therefore, the tendon forces are derived from the optimization calculation of the following equation [59]:

$$u(F_{tendon}) \triangleq \sum_{i=1}^{n} \left(\frac{f_i}{PCSA_i} \right)^2 \rightarrow \min \tag{4.19}$$

$$0 \leq f_i \leq f_{imax} \tag{4.20}$$

where $PCSA$ is a physiological cross sectional area of each muscle and f_{max} is a maximal force of each muscle that is determined by $PCSA$ and maximal muscle stress [60]. In this thesis, we used the $PCSA$ values of Cuevas *et al.* research [57][58] (Table 4.1).

Table 4.1. PCSA [cm^2] of each muscles [57][58]

FDP	FDS	EIP	EDC	LUM	DI	PI
4.1	3.65	1.12	1.39	0.36	4.16	1.6

FPL	FPB	EPL	EPB	APL	APB	ADPt	ADPo	OPP
2.08	0.66	0.98	0.47	1.93	0.68	2.0	2.0	1.02

4.4 Summary

This chapter explained the calculation method of the grasp effort score using the tendon force margin. The calculation flow of the grasp effort score was shown. The score is calculated from the grasp force using the tendon skeletal model of the index finger and the thumb. Next, the vision based grasp force control method was explained. This force control method is based on the incipient slip information of the fingertip. Then the tendon skeletal model and the finger posture estimation method were explained. The tendon skeletal model is constructed based on human moment arm data.

Chapter 5

Grasp effort evaluation via simulation

In this chapter, the validity of the proposed method by comparing simulation results with the human experimental results. We show two experiments that are pinching object and pushing cell-phone button. The scores of these operation are calculated using the proposed grasp effort estimation. We show that the simulation results are similar to the human experiment results.

5.1 Pinching cylinder simulation

5.1.1 Simulation condition of pinching cylinders

In this simulation, we use the condition as same as the human experiment in sec. 3. Dimension of the cylinders are 20, 40, 60, 80 and 100 [mm] in length and 20 [mm] in diameter. Weight of the cylinder is 600 [g]. The cylinder is pinched in the length direction by both the index finger and the thumb. Table 5.1 shows the finger model parameters and table 5.2 shows the limit angle of each joint. The finger link parameters are given based on the measurement of that of the subject. The contact points are the fingertip of each finger and the center of the cylinder. The friction coefficient is set as $\mu = 0.5$ and the fingertip force is set as 11.76 [N]. The vectors from the DIP/IP joint to the load point are $\mathbf{P_I} = \left\{ \begin{array}{ccc} 10.0 & 5.0 & 0.0 \end{array} \right\}^T$ and $\mathbf{P_T} = \left\{ \begin{array}{ccc} 17.0 & 5.0 & 0.0 \end{array} \right\}^T$.

Table 5.1. Link sizes [mm]

l_{I1}	l_{I2}	l_{I3}	l_{I4}	l_{T1}	l_{T2}	l_{T3}	l_{T4}
39.0	25.0	10.0	5.0	45.0	32.0	17.0	5.0

5.1.2 Simulation results of pinching cylinders

Fig. 5.1 shows the each estimated tendon force of the index finger and the thumb when pinching the cylinders. The tendon forces of the thumb ADPt becomes higher according to the cylinder length. On the other hand, the tendon forces of the index finger FDS becomes lower according to the cylinder length. This result indicates a possibility that the quantitative evaluation using the tendon force. The pattern of these tendon forces is similar to the human muscle activity shown in Fig. 3.8 and Fig. 3.9. This results suggest that the finger model can simulate human muscle activity. The score of each cylinder length was calculated from these tendon forces using Eq. 4.1.

Fig. 5.2 shows the evaluated score by the simulation and human questionnaire result. The curves in the figure are the approximate quadratic curve of the result. The lowest score is observed in the 60 [mm] cylinder length. On the other hand, the highest score is observed in 20 [mm] cylinder length. The simulated score pattern is similar to the human questionnaire score pattern. The correlation coefficient between the simulated score and the questionnaire score of human is 0.97. There is strong correlation (the p-value is 0.007). This indicates that the

Table 5.2. Limit angle

	flexion(adduction)	extension(abduction)
θ_{I1} [degree]	-60	0
θ_{I2} [degree]	-25	15
θ_{I3} [degree]	-75	0
θ_{I4} [degree]	-60	0

	flexion(adduction)	extension(abduction)
θ_{T1} [degree]	-20	25
θ_{T2} [degree]	-20	20
θ_{T3} [degree]	-60	10
θ_{T4} [degree]	-15	15
θ_{T5} [degree]	-60	20

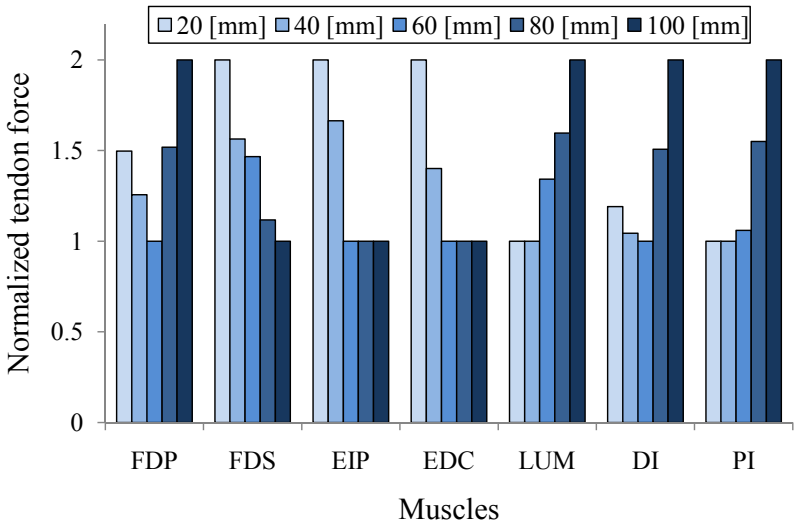

(a) Muscle of the index finger

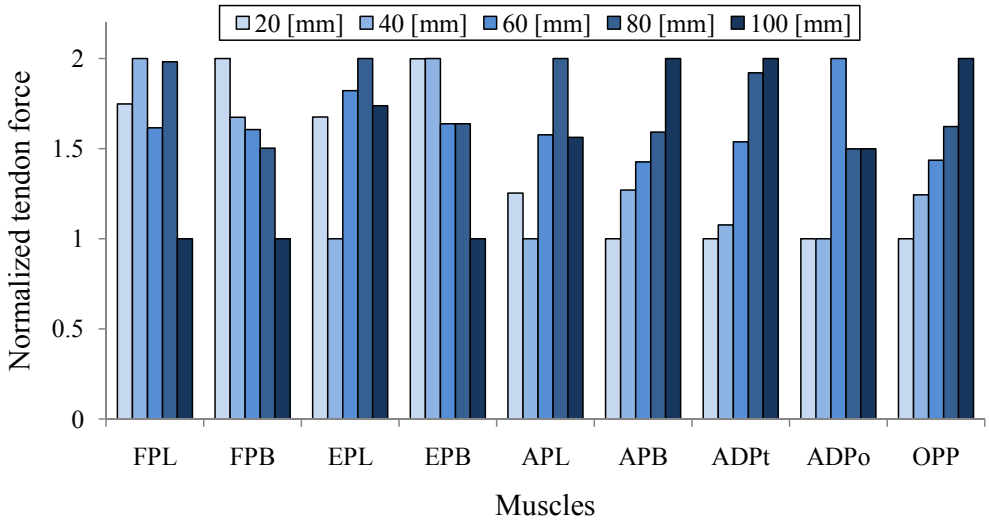

(b) Muscle of the thumb

Figure 5.1. Simulation results

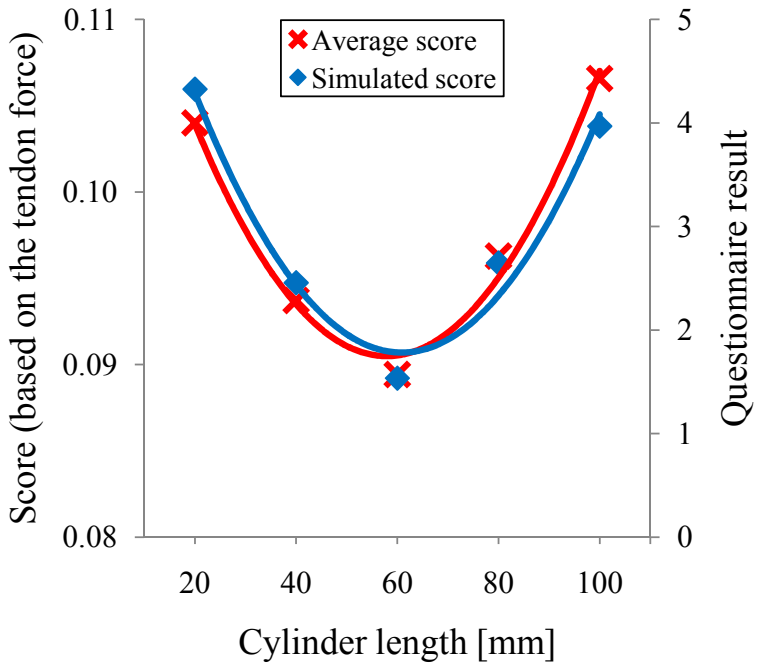

Figure 5.2. Simulation scores

proposed method can reflect human subjective pinching effort.

Fig. 5.3 to Fig. 5.12 show the finger postures of the simulation and human when pinching the 20 [mm] to 100 [mm] cylinder respectively. The lines of the human finger posture are virtual links based on the pictures joints. We can see that the estimated finger postures are similar to the human finger postures. Table 5.3 shows the simulated joint angles and table 5.4 shows the measurement joint angles of human. Fig. 5.13 to Fig. 5.17 show the joint angles of the simulated joint angles and the measured finger angles when pinching the 20 [mm] to 100 [mm] cylinder respectively. The lines in the figure are the standard deviation of the measured joint angles. There are no results of the MP AA angle and the IP FE angle, because the CyberGlobe can not measured these joint angle directions. In the simulation, the most efficient posture to exert fingertip force is that AA directions of each joint are zero. The human finger postures are different from the simulation results (see θ_{I2} and θ_{T2} in table 5.4). This cause is a modeling error and a measurement error. However, there are strong correlation between the simulated joint angles and the measured joint angles. Table 5.5 shows the

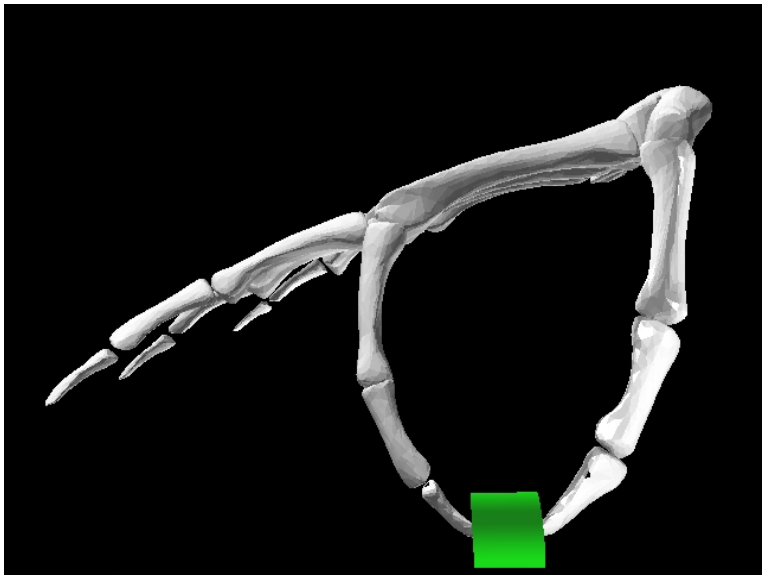

Figure 5.3. Simulation result (20 [mm])

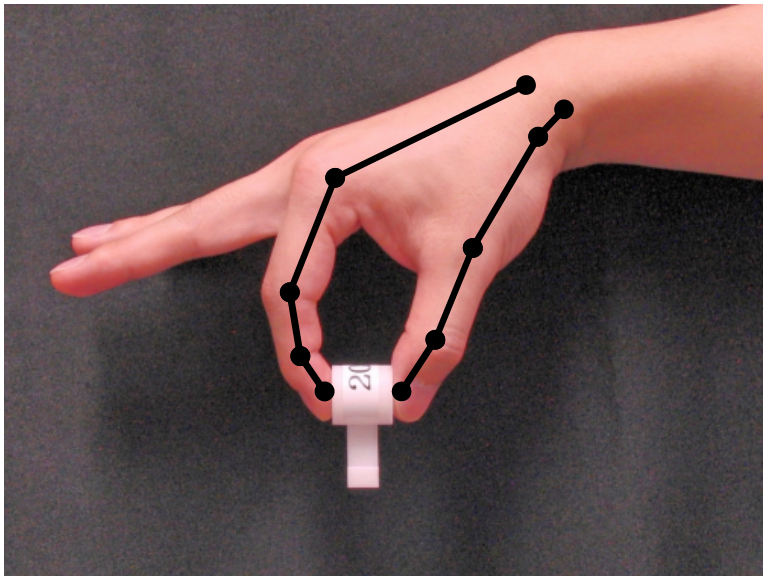

Figure 5.4. Human posture (20 [mm])

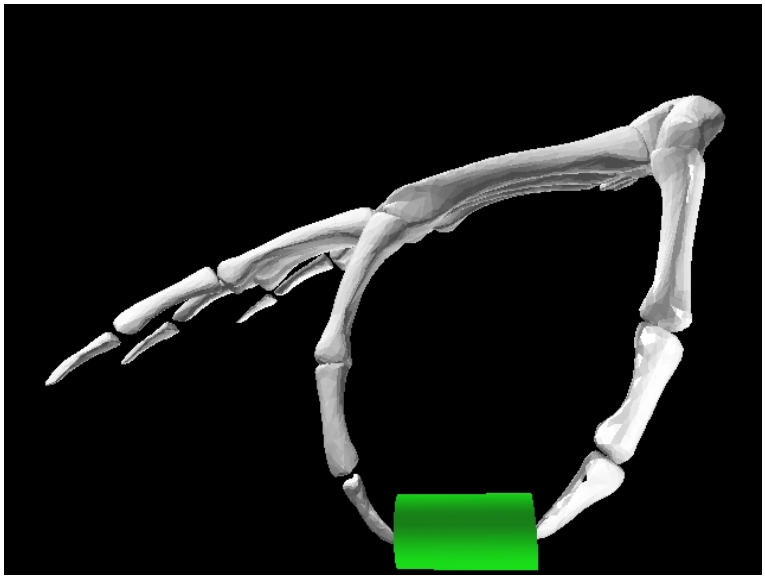

Figure 5.5. Simulation result (40 [mm])

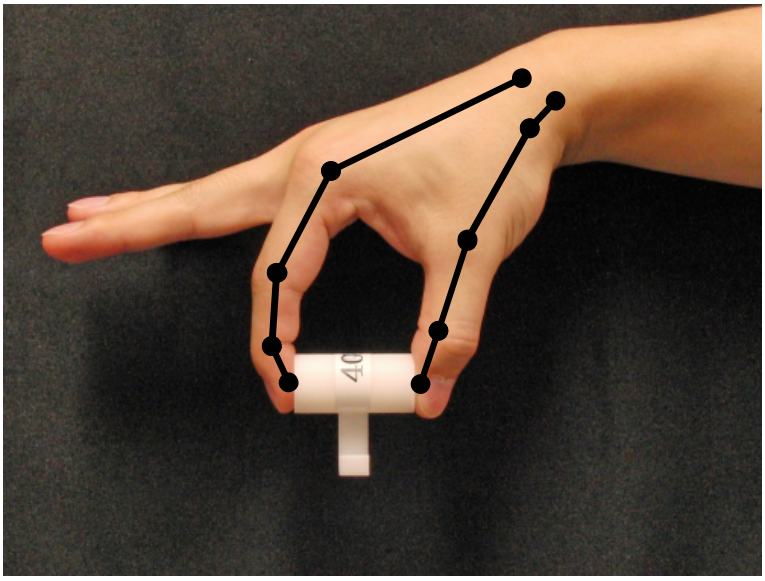

Figure 5.6. Human posture (40 [mm])

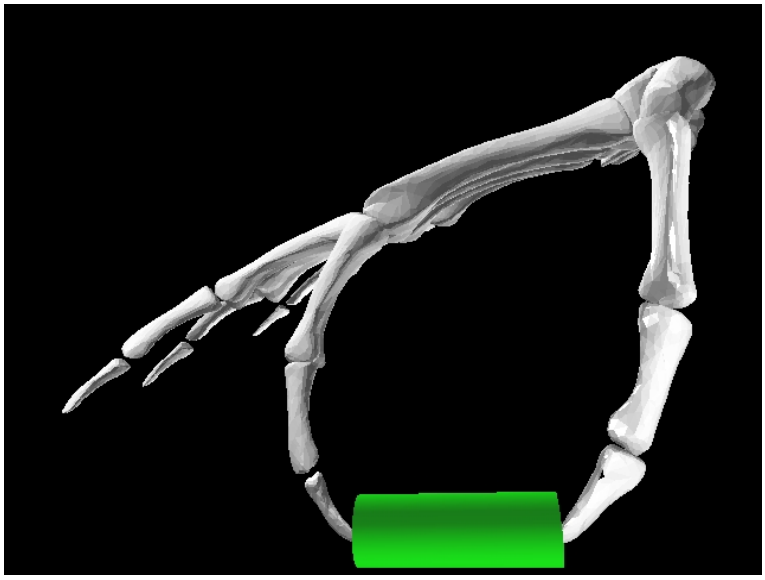

Figure 5.7. Simulation result (60 [mm])

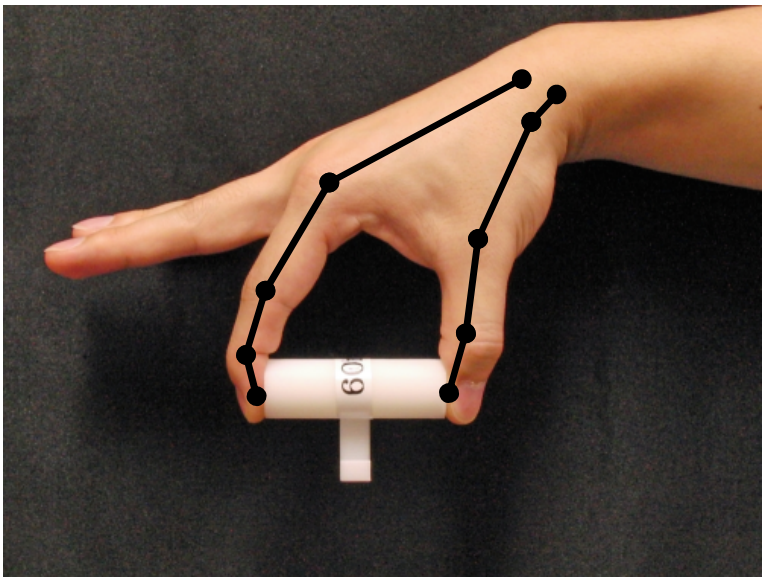

Figure 5.8. Human posture (60 [mm])

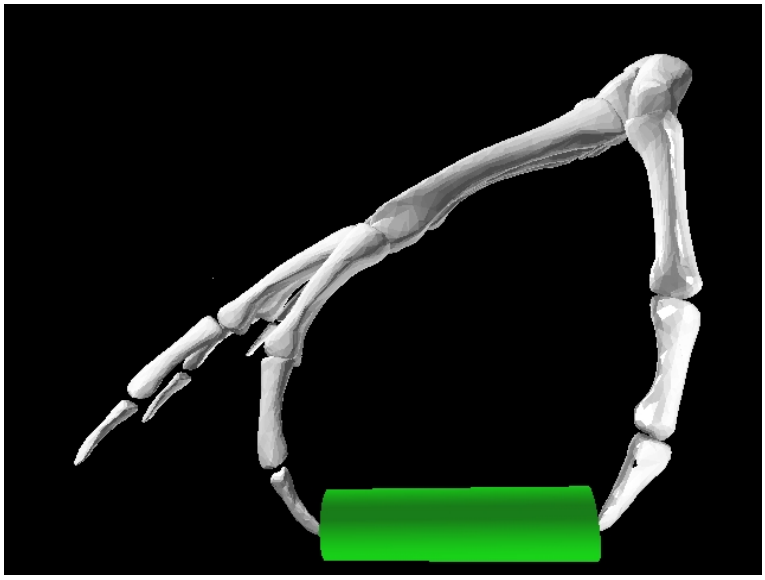

Figure 5.9. Simulation result (80 [mm])

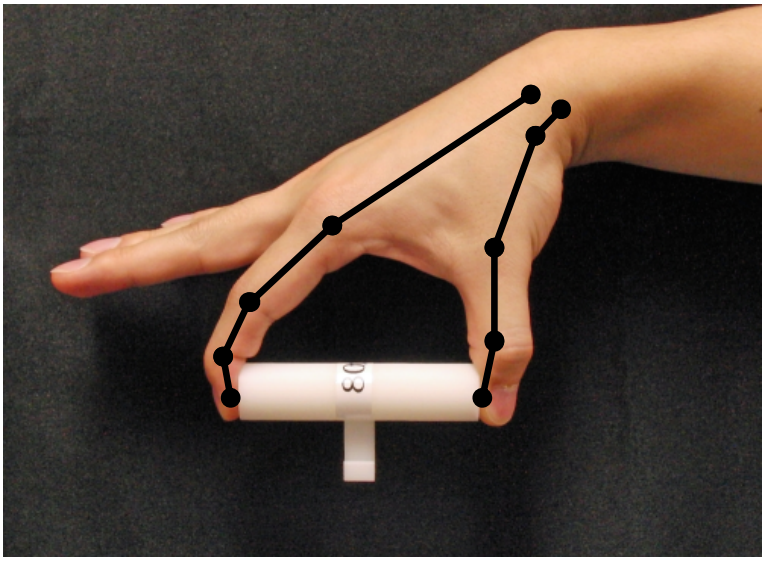

Figure 5.10. Human posture (80 [mm])

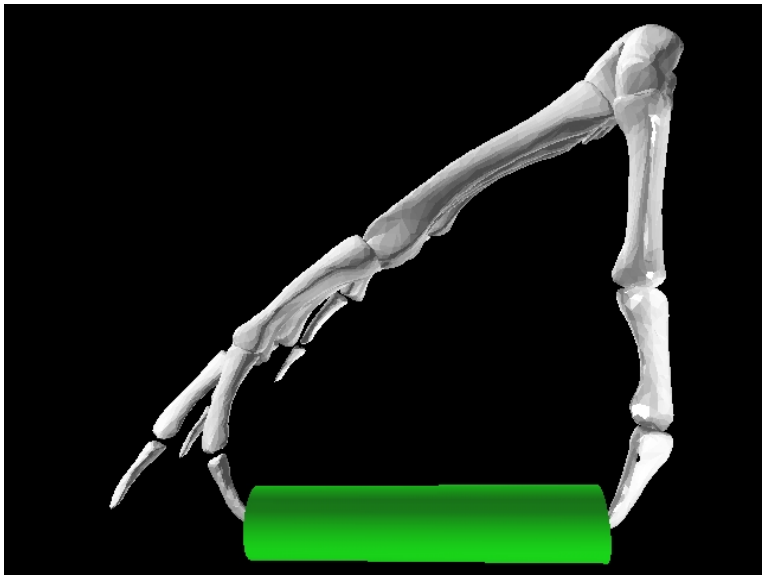

Figure 5.11. Simulation result (100 [mm])

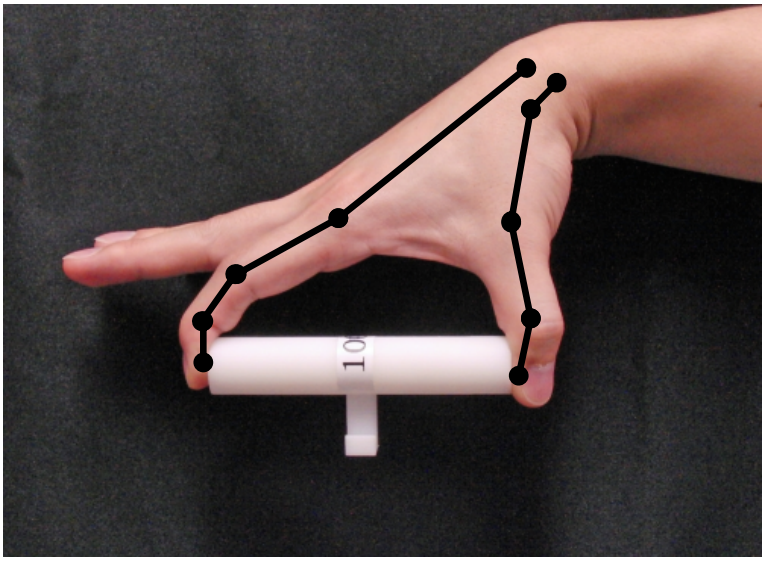

Figure 5.12. Human posture (100 [mm])

Table 5.3. Simulated joint angle ([deg])

Cylinder length	θ_{I1}	θ_{I2}	θ_{I3}	θ_{I4}
20 [mm]	-60.0	0.0	-18.5	-11.9
40 [mm]	-51.2	0.0	-24.3	-17.0
60 [mm]	-37.8	0.0	-20.7	-21.5
80 [mm]	-19.5	0.0	-25.6	-26.5
100 [mm]	-2.3	0.0	-19.4	-29.7

Cylinder length	θ_{T1}	θ_{T2}	θ_{T3}	θ_{T4}	θ_{T5}
20 [mm]	-3.8	0.0	-3.0	0.0	-5.1
40 [mm]	4.0	0.0	-10.1	0.0	-7.2
60 [mm]	5.1	0.0	-0.1	0.0	-11.0
80 [mm]	9.3	0.0	-4.9	0.0	-11.2
100 [mm]	14.4	0.0	-3.1	0.0	10.8

Table 5.4. Measured joint angles ([deg])

Cylinder length	θ_{I1}	θ_{I2}	θ_{I3}	θ_{I4}
20 [mm]	-62.5	-6.8	-23.6	-5.6
40 [mm]	-51.6	-4.8	-27.0	-9.5
60 [mm]	-21.8	-0.6	-15.9	-17.6
80 [mm]	-8.1	-3.2	-18.3	-23.6
100 [mm]	14.2	-7.1	-17.3	-31.2

Cylinder length	θ_{T1}	θ_{T2}	θ_{T3}	θ_{T4}	θ_{T5}
20 [mm]	-4.5	8.5	-5.0	-	-
40 [mm]	0.4	14.8	-10.6	-	-
60 [mm]	12.3	-1.8	-10.6	-	-
80 [mm]	16.3	-7.3	-10.6	-	-
100 [mm]	15.5	-11.7	-11.0	-	-

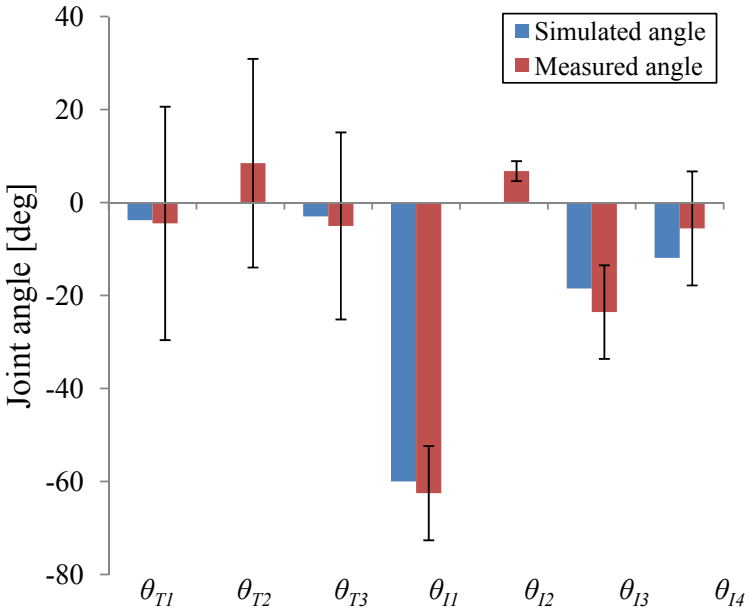

Figure 5.13. Comparison of the joint angles (20 [mm])

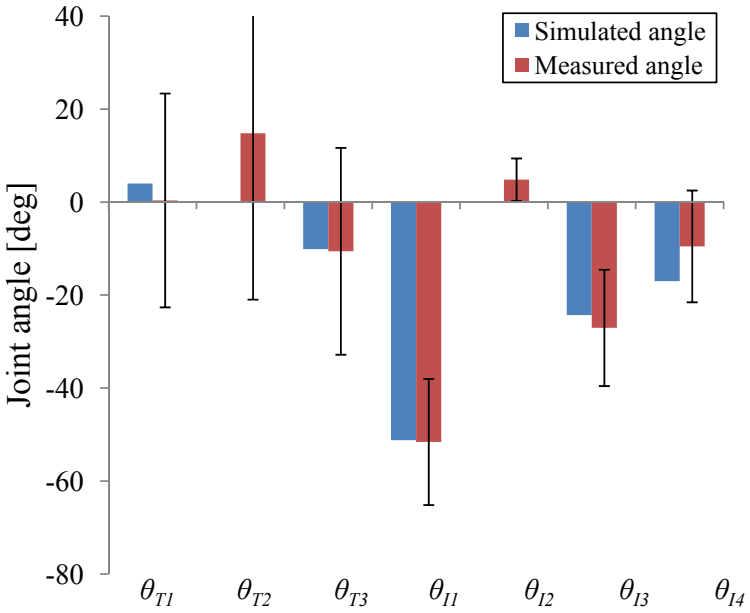

Figure 5.14. Comparison of the joint angles (40 [mm])

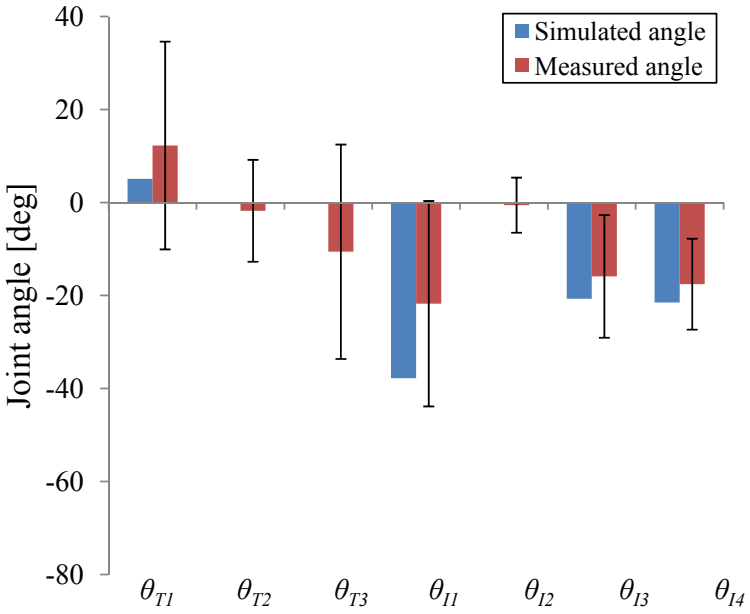

Figure 5.15. Comparison of the joint angles (60 [mm])

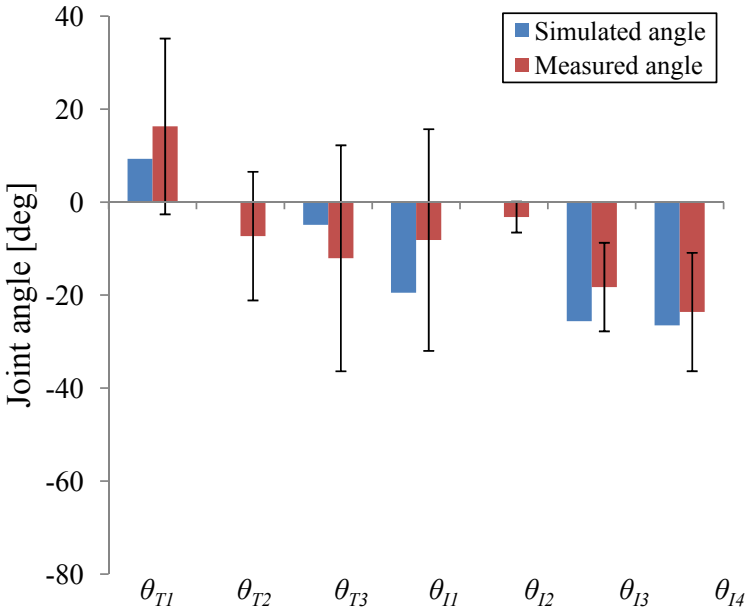

Figure 5.16. Comparison of the joint angles (80 [mm])

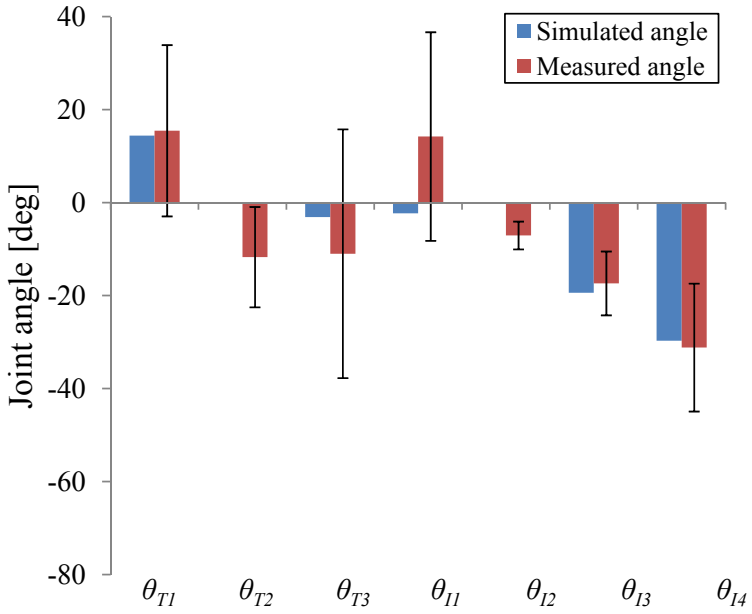

Figure 5.17. Comparison of the joint angles (100 [mm])

Table 5.5. The correlation coefficient of the joint angles

	20 [mm]	40 [mm]	60 [mm]	80 [mm]	100 [mm]
Correlation coefficient	0.98	0.96	0.87	0.85	0.83
P-value	$\ll$0.001	$<$0.001	0.012	0.016	0.020

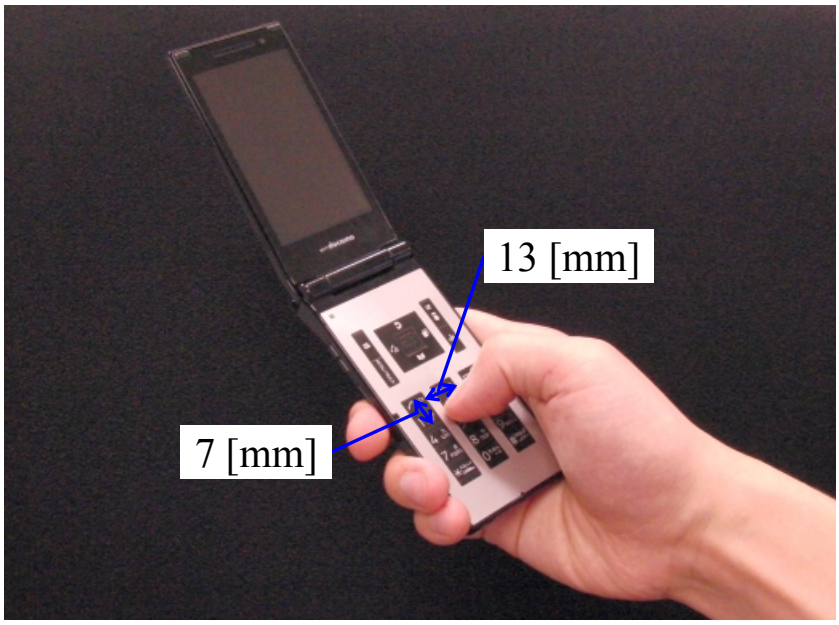

Figure 5.18. Experiment overview of pushing cell-phone button

correlation coefficients and the p-value when pinching the 20 [mm] to 100 [mm] cylinder respectively. The error average of the all joint angle is 5.86 [deg] and the standard deviation of the error is 4.40 [deg]. These results show that the estimated finger posture is enough to use the grasp force estimation.

5.2 Application for button pushing evaluation

5.2.1 Simulation condition of pushing cell-phone buttons

We show an application of the proposed method that is to pushing effort evaluation of cell-phone buttons. First, we measure human subjective effort of pushing cell-phone button by a questionnaire survey. Fig. 5.18 shows an overview of the experiment. Ten healthy male subjects, aged 22 to 30 years old, volunteered for the experiment. All subjects were given the experimental detail and they gave their consent to participate. The pinching motion was conducted by their dominant arm. The button pitches are 13 [mm] in column direction and 7 [mm] in row direction. In the experiment, the subjects pushed each button and scored the effort level of the pushing button. The score had nine levels from 1: "very easy

to push" to 9: "very difficult to push". The subjects push a button in arbitrary order.

Second, the pushing button scores are calculated using a simulation. The button pitch of the simulation is measured from a real cell-phone and the force of the pushing button is set as 2 [N].

Finally, we estimate the pushing button scores when we change the cell-phone button layout to widely. The button pitch of the wide layout is set as double pitch of the standard layout and the pushing force is as same as before.

5.2.2 Simulation results of pushing cell-phone buttons

Fig. 5.19 shows the questionnaire result of human and Fig. 5.20 shows the simulated scores. The correlation coefficient between the simulated score and the questionnaire score of human is 0.68. There is correlation between the simulated score and the questionnaire score of human (the p-value is 0.046). These results show that the scores of the buttons close the thumb origin are difficult to pinch than that of the buttons far from the origin. The simulated scores can be reflected human subjective effort.

Fig. 5.21 and Fig. 5.22 show the standard and wide layout of the cell-phone button and the reachable range of the thumb, respectively. The blue area in this figure is the reachable range of the thumb, the blue triangle marks are the thumb origin, and the red cross marks are the contact points of each button. Fig. 5.23 and Fig. 5.24 show the estimated finger postures when using the standard button layout and when using the wide button layout, respectively. The lines in this figure are the thumb link and the blue triangle marks are the thumb origin. The thumb link colors in this figure change according to the score, the red line means that the score is bad, the blue line means that the score is good. The total score of the standard button layout is 42.9 and the wide button layout is 45.4. This means the standard button layout is easier to use than the wide button layout. These results indicate a possibility that we can estimate product usability using the proposed method.

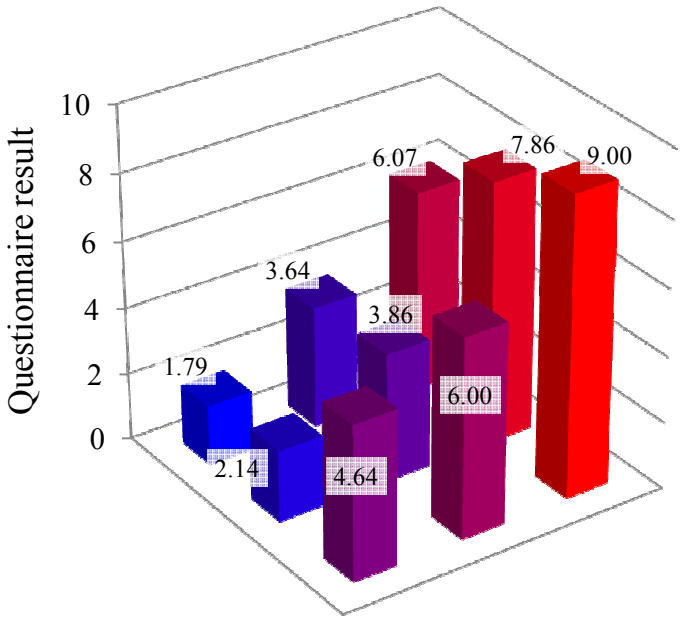

Figure 5.19. Human questionnaire result

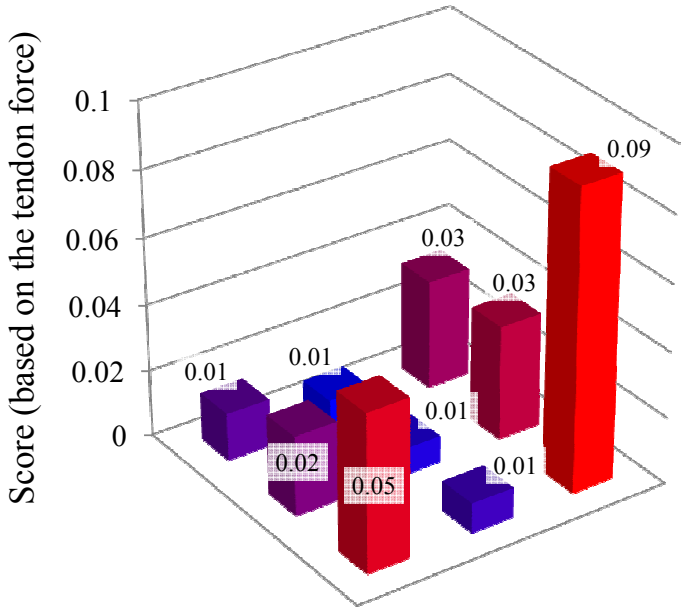

Figure 5.20. Simulated score of pushing button

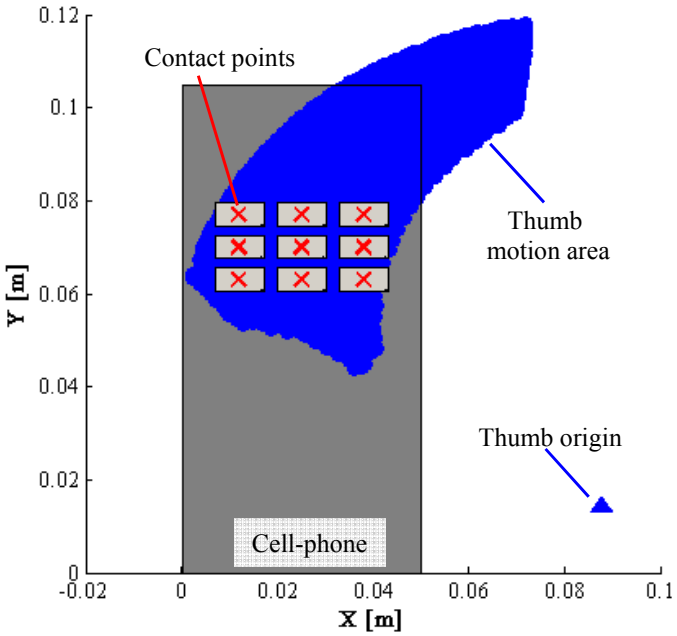

Figure 5.21. Standard button layout

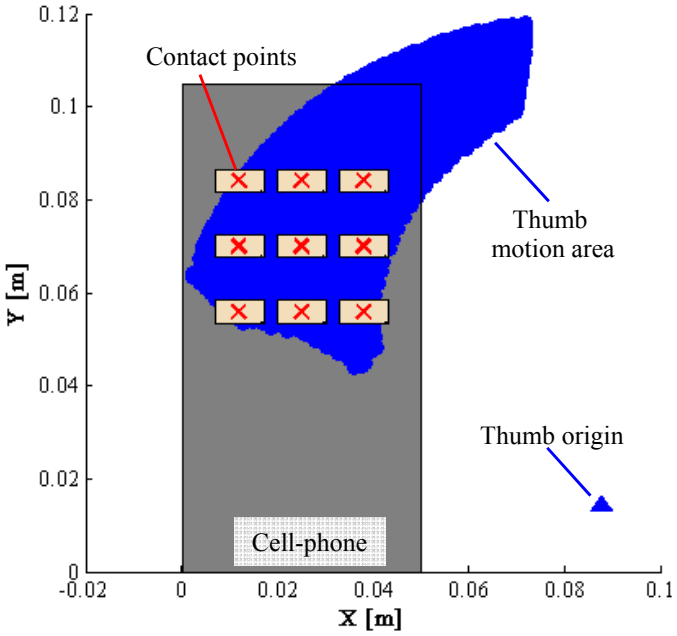

Figure 5.22. Wide button layout

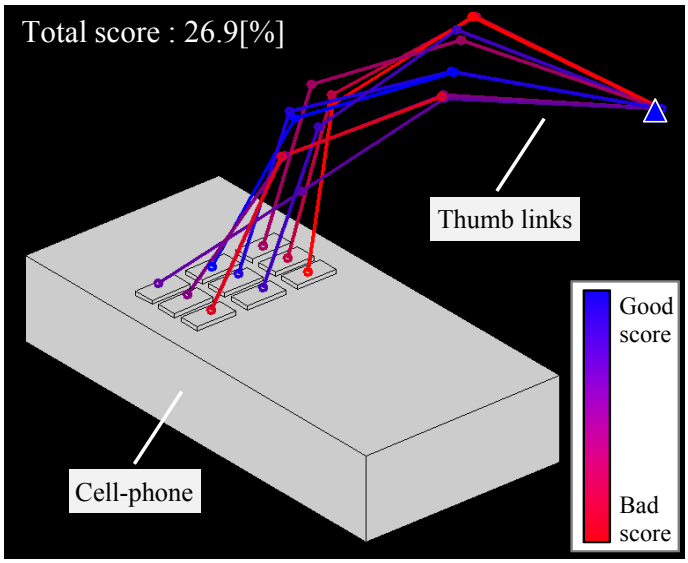

Figure 5.23. Thumb posture of standard button layout

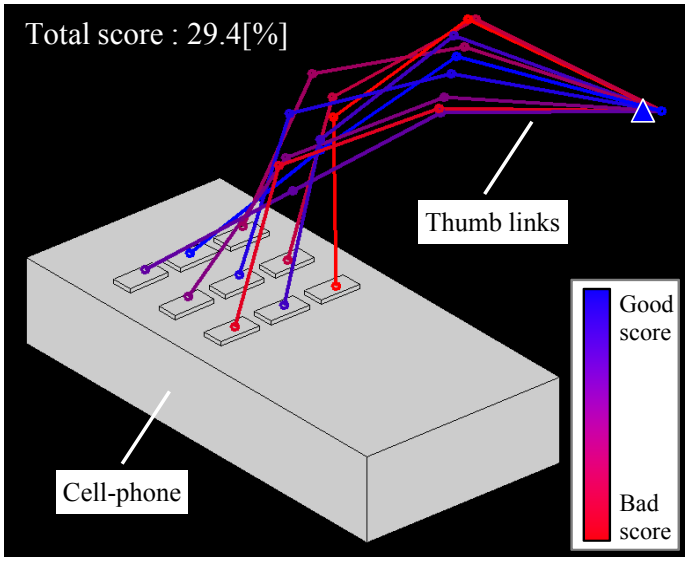

Figure 5.24. Thumb posture of wide button layout

5.3 Summary

This chapter showed the evaluation experiment of the effort in the case of pinching a cylinder and pushing a cell-phone button. At first, the simulated score when pinching cylinders is compared with the questionnaire survey result of human. This experimental results show that the simulated score is similar to the questionnaire survey results and the estimated finger posture is also similar to the human finger posture. Second, an application of the proposed method that is to pushing effort evaluation of cell-phone buttons was shown. The simulated score when pushing cell-phone button is compared with the questionnaire survey result of human. This experimental results show that the simulated score is similar to the questionnaire survey results. And, the standard button layout, which is commonly used in the commercial cell-phone is compared with another layout where the pitch is wider. This comparison clarifies that the standard layout is better than the wide layout. These results showed that the proposed evaluation method can be use for the quantitative evaluation of the product usability.

Chapter 6

Grasp effort evaluation via robot finger

In this chapter, we develop a robot hand as a prototype of the sensing hand to show the possibility of product usability evaluation using a robot hand. We show a detail of the robot hand that made from a tendon-driven hand model and control system. And we compare the experimental result of pinching a cylinder with the human questionnaire result.

6.1 Human like robot finger

6.1.1 Robot system

Fig. 6.1 shows the developed human-like robot arm and hand used as a prototype of the sensing hand. The robot hand is made from the finger-flex mechanism model (M170, SAKAMOTO MODEL). This model teaches us a human tendon's skeletal structure. The thumb has only one degree of freedom in the DIP joint, and the other fingers have 3 degrees of freedom in the DIP, the PIP, and the MCP joints. The model has a total of 13 degrees of freedom. The dimensions of the robot hand are shown in Table 6.1.

Each joint of the hand is wire-driven, and we implemented Dynamixel motors (DX117, Robotis) to drive the joints. Each motor is controlled by a computer

Table 6.1. Robot hand dimensions

Hand length [mm]	185.0
Palm length [mm]	96.0
Hand breadth [mm]	77.0
Thumb length [mm]	59.0

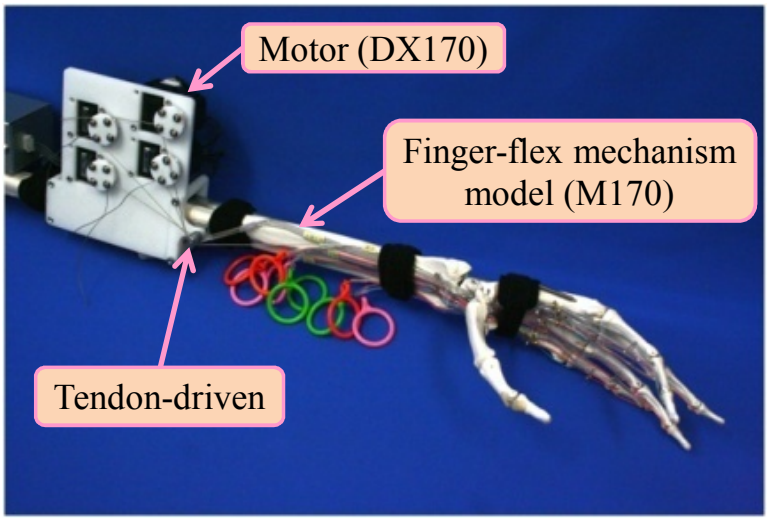

Figure 6.1. Tendon-driven robot hand

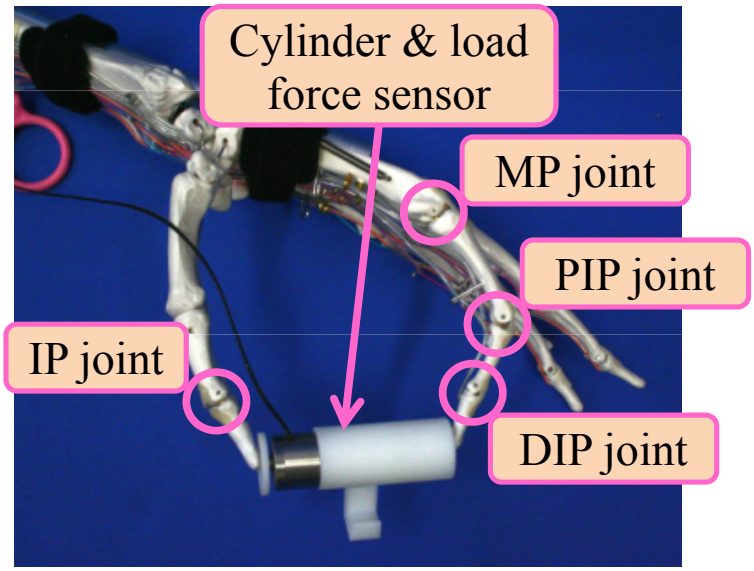

Figure 6.2. Experiment with robot hand

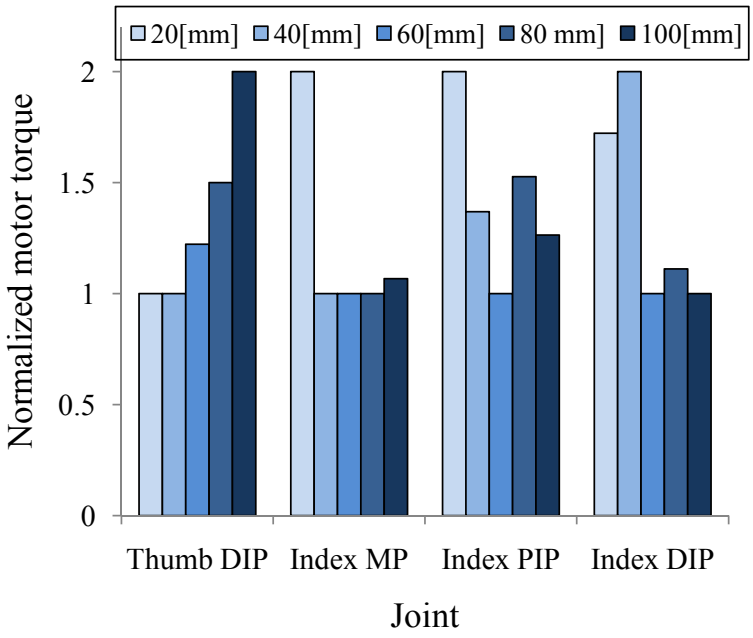

Figure 6.3. Motor torques of the robot hand

through a serial communication (RS232C). The motor torque of the hand can be assumed to be the same as that of human muscle activity. The motor torque during the pinching motion can measure using the motor's load monitoring function.

Fig. 6.2 shows an overview of the experiment when the robot hand is pinching the 60 [mm] long cylinder. The posture of the robot hand is adjusted to the same posture as that of humans. The pinching experiment was conducted using five cylinders from 20 [mm] to 100 [mm]. We measured the motor torque when the pinching force was 1.0 [N].

6.1.2 Experimental results

Fig. 6.3 shows the moot torque when pinching each cylinder and Fig. 6.4 shows the score based on the motor torques and human questionnaire result. The score is the summation of all motor torques of the index finger and the thumb. The curves in Fig. 6.4 are the approximate quadratic curve of the result.

The motor torque of the thumb becomes higher according to the cylinder length. On the other hand, the motor torque of the index finger becomes lower

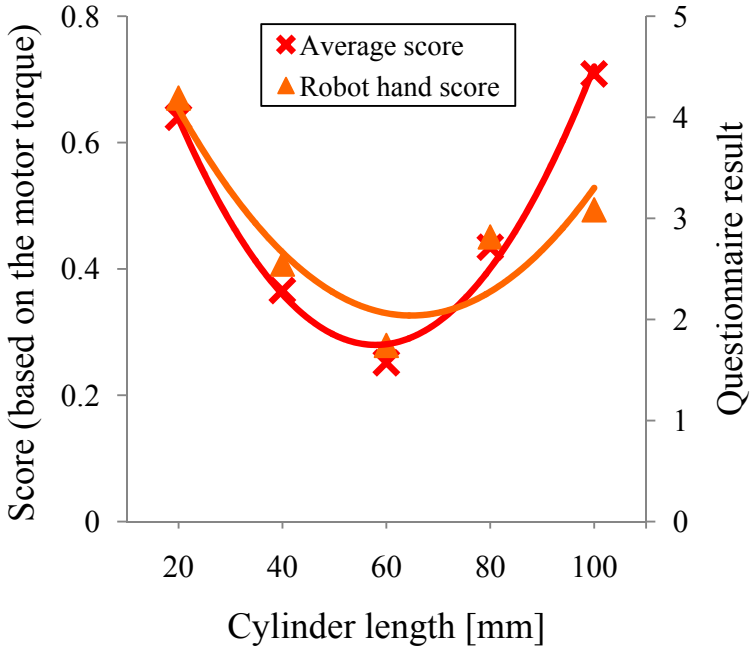

Figure 6.4. Robot hand scores

according to the cylinder length. This pattern is similar to the human muscle activity shown in Fig. 3.8 and Fig. 3.9. A possible reason is that the force transmission efficiency changes according to the moment arm, depending on the joint angle. And the lowest score is observed in the 60 [mm] cylinder length. The robot hand score pattern is similar to the human questionnaire score pattern in Fig. 3.6. The correlation coefficient between the score based on the motor torques and the questionnaire score of human is 0.82. There is correlation between the score based on the motor torque and the questionnaire score of human (the p-value is 0.088). The possible reason of the high p-value ($p > 0.05$) is that the robot hand structure is not enough to evaluate the grasp effort. These experimental results show that the robot hand closely reflects human muscle activity to evaluate human subjective effort. Consequently, this finding is useful for quantitatively evaluating pinching effort.

6.2 Summary

This chapter discussed about a sensing hand prototype that is made from the finger-flex mechanism model. The motor torque of the robot hand can be assumed to represent the human muscle activity. In the experiment, the motor torque of the robot hand was measured when the hand pinches cylinders with length from 20 [mm] to 100 [mm]. Experimental results show that the profile of the motor torque has similar characteristics to that of human muscle activity. These experimental results show that the robot hand closely reflects human muscle activity to evaluate human subjective effort.

Chapter 7

Conclusion and Future works

Summary

This thesis aims to design an evaluation system of grasp effort using both a simulation and a robot hand that are equipped with multiple sensors, such as contact sensors, pressure sensors, and force sensors.

At first, we showed the importance of the tendon forces to evaluate grasp effort by human experiment. The experimental results of human pinching cylinder are shown: the subjective pinching effort, the pinching force, the human EMG and the finger posture. These experimental results mean that the integrated surface EMG is one of the important indexes to indicate grasp effort. This indicates a possibility that the quantitative evaluation using the muscle or tendon force.

Second, the score calculation method of the grasp effort using the tendon force was explained. The calculation flow of the grasp effort score was shown. The score is calculated from the grasp force using the tendon skeletal model of the index finger and the thumb. Next, the vision based grasp force control method was explained. This force control method is based on the incipient slip information of the fingertip. Then the tendon skeletal model and the finger posture estimation method were explained. The tendon skeletal model is constructed based on human moment arm data.

Third, we showed the evaluation experiment of the effort in the case of pinching a cylinder using the simulation. The simulated score using the proposed method is compared with the human questionnaire result. The experimental results show that the simulation score is similar to the questionnaire survey results and the estimated finger posture is also similar to the human finger posture. And, the pushing effort of the cell-phone button is evaluated as a application of the proposed method. The simulated score was compared with the human questionnaire result. This result showed that the simulated scores can be reflected human subjective effort. The standard button layout, which is commonly used in the

commercial cell-phone is compared with another layout where the pitch is wider. This comparison clarifies that the standard layout is better than the wide layout. These results indicate a possibility that we can estimate product usability using the proposed method.

Finally, a prototype of a sensing hand that can measure the tendon force of fingers was developed using a tendon-driven hand model. The motor torque of the robot hand can be assumed to represent the human muscle activity. In the experiment, the motor torque of the robot hand was measured when the hand pinches cylinder. Experimental results show that the profile of the motor torque has similar characteristics to that of human muscle activity. These experimental results show that the robot hand closely reflects human muscle activity to evaluate human subjective effort.

Future work and vision

In this thesis, we developed the index finger and the thumb model for the evaluation system. These model can be used for the product evaluation using each finger or both. We can evaluate more operation to add another fingers (the middle, the ring and the small finger). We need biomechanical analyzation of human finger structure to construct these finger models.

The muscle activity during dynamic motion is different from the static situation. We can use the proposed method when we evaluate a motion that slowly or insensible. The dynamic model of finger and muscle are needed to evaluate a dynamic product operation.

In addition, finger model personalization is interesting work. The proposed method can show product usability of one person by using personal model. The estimation method of finger model parameter that we can use without anatomy is necessary.

We focused only on tendon force, but tactile sensation takes also very important to decide the product usability for humans. In this thesis, we propose the grasp force control method based on the incipient slip information. It is important for more accurate evaluation to analyze a relationship between the tactile sensation and the human subjective effort.

Future work includes developing a sensing hand that can measure the tendon

force, the contact force and the tactile information. The sensing hand should mimic a human tendon skeletal structure. We have to analyze the detail of the tendon movement and the tendon function during finger motion.

Acknowledgements

I would like to express my gratitude and special thanks to Professor Tsukasa Ogasawara for all his support and guidance over the past eight years and throughout my stay and not stay in his laboratory at NAIST. I would also like to special thank that he lead me to the academic career.

My deepest gratitude goes to Professor Kouichi Nishitani of NAIST for sparing me his precious time to evaluate my work with interest.

Many thanks go to Associate Professor Jun Takamatsu of NAIST for his support and accurate advice about the research direction and the methods adopted to solve the considered problem.

Particular thanks go to Assistant Professor Yuichi Kurita of NAIST for his support and fruitful discussions about the research details and to check many my writings.

Special thanks go to Assistant Professor Kentaro Takemura of NAIST for his support and good advice about the research direction.

Particular thanks go to Assistant Professor Jun Ueda of Georgia Institute of Technology for pushing me toward biomechanical system.

Many thanks go to Dr. Yoshio Matsumoto of National Institute of Advanced Industrial Science and Technology for excellent advice about the research approach.

Much appreciation goes to Dr. Mitsunori Tada of Digital Human Research Center and Dr. Kazuyuki Nagata of National Institute of Advanced Industrial Science and Technology for fruitful discussions about the research direction and the aspect of experimental results.

I am thankful Associate Professor Etsuko Ueda of Nara Sangyo University (currently at Nara National College of Technology), Associate Professor Masanao Koeda of Osaka Electro-Communication University and Dr. Jyunichi Ido of National Institute of Advanced Industrial Science and Technology Dr. Tsuyoshi Suenaga, Mr. Albert Causo and Dr. Ding Ming for their friendship and their support during the particularly depressing moments. Without their help many parts of this work would not have been accomplished property.

Many thanks go to Secretary Megumi Kanaoka, Miyuki Yamaguchi and Michiyo

Owaki of Robotics laboratory at NAIST for their support to process many kinds of paperwork, and for their kind help throughout my stay.

All my heartfelt appreciation goes to the current and previous students of Robotics laboratory at NAIST for their help and kindness. Without them I would not have enjoyed my stay thoroughly.

I would like to thank to Mr. Takashi Kaieda and the current and previous members of IM Company Robot Business Division at Yamaha Motor Co., LTD. for cheering me up during my stay.

I would like to thank to Japan Society for the Promotion of Science (JSPS) for supporting me financially in last two years.

Special thanks to all my friends for the moral support, their patience during my difficult moments and their cheerfulness during joyful ones.

I wish to thank my parents and family, whose unwavering love and support goes beyond limits and provides me with strength to pursue my studies.

To my wife Miki and our baby, all I can say is it would take another thesis to express my deep love for you. Your patience, love and encouragement have upheld me.

References

[1] FANUC, http://www.fanuc.co.jp/.

[2] YASKAWA, http://www.yaskawa.co.jp/.

[3] KAWASAKI, http://www.khi.co.jp/robot/.

[4] JISB0134, "Manipulating industrial robots - vocabulary," 1998.

[5] F. Reuleaux, "The kinematics of machinery," *Macmillan, New York*, 1876, republished by Dover, New York, 1963.

[6] Y. Endo, S. Kanai, T. Kishinami, N. Miyata, M. Kouchi, and M. Mochimaru, "Virtual grasping assessment using 3d digital hand model," in *Proceedings of 10th Annual Applied Ergonomics Conference*, 2007.

[7] S. Sugiyama, M. Koeda, H. Fujimoto, and T. Yoshikawa, "Measurement of grasp position by human hands and grasp criterion for two soft-fingered robot handsl," in *Proceedings of the 2009 IEEE international conference on Robotics and Automation (IEEE ICRA 2009)*, 2009, pp. 1127–32.

[8] M. T. Ciocarlie and P. K. Allen, "Hand posture subspaces for dexterous robotic grasping," *International Journal of Robotics Research*, vol. 28, no. 7, pp. 851–67, 2009.

[9] C. Goldfeder, M. T. Ciocarlie, H. Dang, and P. K. Allen, "The columbia grasp database," in *Proceedings of the 2009 IEEE international conference on Robotics and Automation (IEEE ICRA 2009)*, 2009, pp. 3343–49.

[10] J. R. Flanagan, M. C. Bowman, and R. S. Johansson, "Control strategies in object manipulation tasks," *Current Opinion in Neurobiology*, vol. 16, no. 6, pp. 650–659, 2006.

[11] K. Terabayashi, N. Miyata, and J. Ota, "Grasp strategy when experiencing hands of various sizes," *Journal of Human Computer Interaction*, vol. 1, no. 4, pp. 55–74, 2008.

[12] A. M. Gordon, G. Westling, K. J. Cole, and R. S. Johansson, "Memory representations underlying motor commands used during manipulation of common and novel objects," *Journal of Neurophysiology*, vol. 69, no. 6, pp. 1789–96, 1993.

[13] A.B. Vallvo and R.S. Johansson, "Properties of cutaneous mechanoreceptors in the human hand related to touch sensation," *Human Neurobiology*, vol. 3, no. 1, pp. 3–14, 1984.

[14] R. S. Johansson and G. Westling, "Coordinated isometric muscle commands adequately and erroneously programmed for the weight during lifting task with precision grip," *Experimental Brain Research*, vol. 71, no. 1, pp. 59–71, 1988.

[15] G. Westling and R. S. Johansson, "Factors influencing the force control during precision grip," *Experimental Brain Research*, vol. 53, no. 2, pp. 277–84, 1984.

[16] R. S. Johansson and G. Westling, "Roles of glabrous skin receptors and sensorimotor memory in automatic control of precision grip when lifting rougher or more slippery objects," *Experimental Brain Research*, vol. 56, no. 3, pp. 550–64, 1984.

[17] ——, "Signals in tactile afferents from the fingers eliciting adaptive motor responses during precision grip," *Experimental Brain Research*, vol. 66, no. 1, pp. 141–54, 1987.

[18] H. Maekawa, K. Tanie, and K. Komoriya, "A finger-shaped tactile sensor using an optical waveguide," in *Proceedings of the 2002 IEEE International Conference on Systems, Man, and Cybernetics*, 1993, pp. 403–8.

[19] N. J. Ferrier and R. W. Brockett, "Reconstructing the shape of a deformable membrane using image data," *International Journal of Robotics Research*, vol. 19, no. 9, pp. 795–816, 2000.

[20] R. D. Howe and M. R. Cutkosky, "Sensing skin acceleration for texture and slip perception," in *Proceedings of the 1989 IEEE international conference on Robotics and Automation (IEEE ICRA 1989)*, 1989, pp. 145–50.

[21] M. R. Tremblay and M. R. Cutkosky, "Estimating friction using incipient slip sensing during a manipulation task," in *Proceedings of the 1993 IEEE international conference on Robotics and Automation (IEEE ICRA 1993)*, 1993, pp. 363–8.

[22] H. Shinoda and S. Ando, "Ultrasonic emission tactile sensor for contact localization and characterization," in *Proceedings of the 1994 IEEE international conference on Robotics and Automation (IEEE ICRA 1994)*, 1994, pp. 2536–43.

[23] T. Maeno, T. Kawai, and K. Kobayashi, "Analysis and design of a tactile sensor detecting strain distribution inside an elastic finger," in *Proceedings of 1998 IEEE/RSJ International Conference on Intelligent Robots and Systems (IEEE IROS 1998)*, 1998, pp. 1658–63.

[24] D. Barker, *The morphology of muscle receptors*, ser. Handbook of Sensory Physiology. Springer, Berlin, 1974, vol. III/2.

[25] D. I. McCloskey, M. J. Cross, R. Honner, and E. K. Potter, "Sensory effects of pulling or vibrating exposed tendons in man," *Brain*, vol. 109, no. 1, pp. 21–37, 1983.

[26] S. C. Gandevia, *Kinesthesia: roles for afferent signals and motor commands*, ser. Handbook of Physiology Section 12 Exercise: Regulation and Integration of Multiple Systems, L. B. Rowell and J. T. Shepherd, Eds. Oxford University Press, 1996.

[27] A. Inmann and M. Haugland, "An instrumented object for evaluation of latelal hand grasp during functional tasks," *Jounal of Medical Engineering & Technology*, vol. 25, no. 5, pp. 207–211, 2001.

[28] T. Ogawa, I. Mihara, T. Yukawa, and T. Nishizawa, "Quantitative evaluation method for grip comfort level of electric shavers (in japanese)," *Panasonic electric works technical report*, vol. 52, no. 3, pp. 24–29, 2004.

[29] M. Saihara, T. Hattori, M. Yoshida, Y. Yamada, and I. Mihara, "Evaluation of usability of rechargeable impact driver (in japanese)," *IEICE technical report. ME and bio cybernetics*, vol. 107, no. 80, pp. 29–32, 2006.

[30] A. A. Amis, "Variation of finger forces in maximal isometric grasp tests on a range of cylinder diameters," *Journal of Biomedical Engineering*, vol. 9, no. 4, pp. 313–20, 1987.

[31] S. Radhakrishnan and M. Nagaravindra, "Analysis of hand force in health and disease during maximum isometric grasping of cylinders," *Medical and Biological Engineering and Computing*, vol. 31, no. 4, pp. 372–376, 1993.

[32] Y. K. Kong and A. Freivalds, "Evaluation of meat-hook handle shapes," *International Journal of Industrial Ergonomics*, vol. 32, no. 2, pp. 13–23, 2003.

[33] Y. K. Kong, B. D. Lowe, S. J. Lee, and E. F. Krieg, "Evaluation of handle design characteristics in a maximum screwdriving torque task," *Ergonomics*, vol. 50, no. 9, pp. 1404–18, 2007.

[34] Y. Nakamura, K. Yamane, Y. Fujita, and I. Suzuki, "Somatosensory computation for man-machine interface from motion capture data and musculoskeletal human model," *IEEE Transactions on Robotics*, vol. 21, no. 1, pp. 58–66, 2005.

[35] MusculoGraphics Inc., "http://www.musculographics.com."

[36] LTD. CYBERNET SYSTEMS CO., "http://www.cybernet.co.jp/anybody/."

[37] Life Modeler Inc., "http://www.lifemodeler.com."

[38] GSport Inc., "http://www.gsport.co.jp/p_l_armo.html."

[39] K. N. An, E. Y. Chao, W. P. Cooney, and R. L. Linscheid, "Normative model of human hand for biomechanical analysis," *Journal of Biomechanics*, vol. 12, pp. 775–788, 1979.

[40] K. R. S. Holzbaur, W. M. Murray, and S. L. Delp, "A model of the upper extremity for simulating musculoskeletal surgery and analyzing neuromuscular control," *Annals of Biomedical Engineering*, vol. 33, no. 6, pp. 829–840, 2005.

[41] J. T. Dennerlein, "Finger flexor tendon forces are a complex function of finger joint motions and fingertip forces," *Journal of hand therapy*, vol. 18, no. 2, pp. 120–7, 2005.

[42] F. J. Valero-Cuevas, "An integrative approach to the biomechanical function and neuromuscular control of the fingers," *Journal of Biomechanics*, vol. 38, pp. 673–684, 2005.

[43] D. G. Kamper, H. C. Fischer, and E. G. Cruz, "Impact of finger posture on mapping from muscle activation to joint torque," *Clinical Biomechanics*, vol. 21, no. 4, pp. 361–369, 2006.

[44] W. Tsang, K. Singh, and E. Fiume, "Musculotendon simulation for hand animation," in *Proceedings of the 2005 ACM SIGGRAPH/Eurographics symposium on Computer animation*, 2005, pp. 319–28.

[45] S. Sueda, A. Kaufman, and D. K. Pai, "Musculotendon simulation for hand animation," *ACM Transactions on Graphics (Proceedings SIGGRAPH)*, vol. 27, no. 3, pp. 775–788, 2008.

[46] T. Maeno, "Relationship between structure of finger tissue and location of tactile receptors (in japanese)," *Transactions of the Japan Society of Mechanical Engineers, C*, vol. 63, no. 607, pp. 881–8, 1997.

[47] K. Kobayashi and T. Maeno, "Relationship between the structure of finger tissue and the location of tactile receptors : 2nd report, method of dynamic contact analysis and results for contact between the finger and plane plate (in japanese)," *Transactions of the Japan Society of Mechanical Engineers, C*, vol. 64, no. 628, pp. 4798–805, 1998.

[48] ——, "Relationship between the structure of finger tissue and the location of tactile receptors : 3rd report, results of contact analysis between a finger and a rough plate (in japanese)," *Transactions of the Japan Society of Mechanical Engineers, C*, vol. 65, no. 636, pp. 3321–7, 1999.

[49] M. Tada and D. K. Pai, "Finger shell: Predicting finger pad deformation under line loading," in *Proceedings of the Symposium on Haptic Interfaces for Virtual Environment and Teleoperator Systems*, 2008, pp. 107–112.

[50] K. L. Johnson, "Contact mechanics," *Cambridge University Press*, 1985.

[51] R. D. Mindlin, "Compliance of elastic bodies in contact," *ASME Transactions on Journal of Applied Mechanics*, vol. 16 of E, pp. 259–68, 1949.

[52] N. Xydas and I. Kao, "Modeling of contact mechanics and friction limit surface for soft fingers in robotics with experimental results," *International Journal of Robotics Research*, vol. 18, no. 8, pp. 941–50, 1999.

[53] S. W. Lee, H. Chenb, J. D. Towlesa, and D. G. Kamper, "Estimation of the effective static moment arms of the tendons in the index finger extensor mechanism," *Journal of Biomechanics*, vol. 41, pp. 1567–1573, 2008.

[54] A. D. Deshpande, R. Balasubramanian, R. Lin, B. T. Dellon, and Y. Matsuoka, "Understanding variable moment arms for the index finger mcp joints through the act hand," in *The second IEEE/RAS-EMBS international Conference on Biomedical Robotics and Biomechatronics (BioRob2008)*, 2008, pp. 776–782.

[55] K. N. An, Y. Ueba, E. Y. Chao, W. P. Cooney, and R. L. Linscheid, "Tendon excursion and moment arm of index finger muscles," *Journal of Biomechanics*, vol. 16, no. 6, pp. 419–425, 1983.

[56] W. P. Smutz, A. Kongsayreepong, R. E. Hughes, G. Niebur, W. P. Cooney, and K. N. An, "Mechanical advantage of the thumb muscles," *Journal of Biomechanics*, vol. 31, no. 6, pp. 565–570, 1998.

[57] F. J. Valero-Cuevas, F. E. Zajac, and C. G. Burgar, "Large index-fingertip forces are produced by subject-independent patterns of muscle excitation," *Journal of Biomechanics*, vol. 31, no. 8, pp. 693–703, 1998.

[58] F. J. Valero-Cuevas, M. E. Johanson, and J. D. Towles, "Towards a realistic biomechanical model of the thumb: the choice of kinematic description may be more critical than the solution method or the variability/uncertainty of musculoskeletal parameters," *Journal of Biomechanics*, vol. 36, no. 7, pp. 1019–1030, 2003.

[59] R. D. Crowninshield and R. A. Brand, "A physiologically based criterion of muscle force prediction in locomotion," *Journal of Biomechanics*, vol. 14, no. 11, pp. 793–801, 1981.

[60] F. E. Zajac, "Muscle and tendon: properties, models, scaling, and application to biomechanics and motor control," *Critical Revievies Biomedical Engineering*, vol. 17, no. 4, pp. 359–411, 1989.

[61] Shrawan Kumar, Ed., *Biomechnics in Ergonomics*, Taylor & Francis, ch. 11, p. 212, 1999.

Appendix

A. Linearly constrained optimization problem

A.1 Karush-Kuhn-Tucker Conditions

The Karush-Kuhn-Tucker conditions (KKT conditions) are used in muscle force design. KKT conditions are a necessary conditions for this general equality-inequality constrained problem which was published by Karush, Kuhn and Tucker at 60 years ago.

At first, let us consider the following nonlinear optimization problem.

$$\begin{aligned} & f(\boldsymbol{x}) \rightarrow \min, \\ & \text{such that} : \begin{cases} g_i(\boldsymbol{x}) \leq 0 \quad (i = 1, \cdots, m); \\ h_j(\boldsymbol{x}) = 0 \quad (j = 1, \cdots, l). \end{cases} \end{aligned} \tag{A.1}$$

where $f(\boldsymbol{x})$ is the objective function to be minimized, $\boldsymbol{x} \in \Re^n$ is the variable vector with n elements. $g_i(\boldsymbol{x})$ are the inequality constraints and $h_j(\boldsymbol{x})$ are the equality constraints. m and l are the number of inequality and equality constraints.

Suppose that $f(\boldsymbol{x})$, $g_i(\boldsymbol{x})$ and $h_j(\boldsymbol{x})$ are continuously differentiable at a point $\bar{\boldsymbol{x}}$. If $\bar{\boldsymbol{x}}$ is a minimum (or local minimum) which satisfies some regularity conditions, such $\boldsymbol{\lambda} \in \Re^m$ and $\boldsymbol{\mu} \in \Re^l$ are exist as following:

$$\nabla_x L(\boldsymbol{x}, \bar{\boldsymbol{\lambda}}, \bar{\boldsymbol{\mu}}) = \nabla_x f(\bar{\boldsymbol{x}}) + \sum_{i=1}^{m} \bar{\lambda}_i \nabla g_i(\bar{\boldsymbol{x}}) + \sum_{j=1}^{l} \bar{\mu_j} \nabla h_j(\bar{\boldsymbol{x}}) = 0; \tag{A.2}$$

$$g_i(\bar{\boldsymbol{x}}) \leq 0, \bar{\lambda_i} \geq 0, \bar{\lambda_i} g_i(\bar{\boldsymbol{x}}) = 0 \quad (i = 1, \cdots, m)); \tag{A.3}$$

$$h_j(\bar{\boldsymbol{x}}) = 0 \quad (j = 1, \cdots, l)). \tag{A.4}$$

A.2 Quadratic Programming Problem

Quadratic programming (QP) problem is a special type of mathematical optimization problem which is to optimize (minimize or maximize) a quadratic function of several variables subject to linear constraints on these variables.

Quadratic programming problem is formulated as:

$$f(\boldsymbol{x}) = \frac{1}{2}\boldsymbol{x}^T\boldsymbol{Q}\boldsymbol{x} + \boldsymbol{c}^T\boldsymbol{x} \rightarrow \min, \tag{A.5}$$
$$\text{such that : } \begin{cases} \boldsymbol{A}\boldsymbol{x} \leq \boldsymbol{b}; \\ \boldsymbol{E}\boldsymbol{x} = \boldsymbol{d}. \end{cases}$$

where $f(\boldsymbol{x})$ is the objective function to be minimized, $\boldsymbol{x} \in \Re^{n\times 1}$ is the variable vector with n elements. $\boldsymbol{Q}$ is a $n \times n$ matrix, $\boldsymbol{c}$ is a $n \times 1$ vector. If the number of inequality and equality constraints are m and l, $\boldsymbol{A}$ and $\boldsymbol{E}$ are $m \times n$ and $l \times n$ matrixes, $\boldsymbol{b}$ and $\boldsymbol{d}$ are $m \times 1$ and $l \times 1$ vectors.

From optimization theory introduced in Appendix A.1, a necessary condition for a point $\boldsymbol{x}$ to be a global minimize is for it to satisfy the KKT conditions. Using the KKT condition, we can find the dual of QP problem is also a QP problem. Using Sequential Quadratic Programming (SQP) algorithm, QP problem can be solved.

B. Relationship between the surface EMG and muscle force

In this research, EMG signal is used to measure the change of muscle force with and without assist. In past research, it has been confirmed that the EMG signal have a close relationship with muscle force. EMG signal and muscle force have same change tendency. Muscle force f can be estimated from EMG signal using following linear relational expression:

$$f = \sigma \cdot S \cdot \mathrm{EMG} \cdot c, \tag{B.1}$$

where σ is the specific tension of muscle tissue for maximum muscle activation, S is the physiological cross-sectional area of muscle, EMG is the EMG signal, normalized to maximum voluntary contraction, and c is a factor for transforming relative EMG into relative muscle force [61]. For a linear EMG/force relationship, this factor is 1. For isometric movement, σ is constant and the change rate of EMG signal EMG is same as muscle force f. Therefore, in this research the change rate was compared with muscle force directly.

C. Approximation parameter of moment arms

This section shows the approximation parameters of the moment arms. The moment arm M_i of each tendons changes according to the joint angle θ (radian). We approximate the moment arms as follow equation:

$$M_i = a_1\theta^4 + a_2\theta^3 + a_3\theta^2 + a_4\theta + a_5. \tag{C.1}$$

The parameters of the approximation are based on the row cadavers data that were measured by An *et al.* and Smutz *et al.* [55][56].

Table C.1. MCP joint FE parameters

	a_1	a_2	a_3	a_4	a_5
FDP	-0.0118	-0.0336	-0.0312	-0.0065	-0.0094
FDS	-0.0332	-0.0802	-0.0632	-0.0131	-0.0102
EIP	0.0039	0.0003	-0.0075	-0.0059	0.0074
EDC	0.0247	0.0381	0.0084	-0.0077	0.0060
LUM	-0.0096	-0.0350	-0.0390	-0.0137	-0.0087
DI	-0.0105	-0.0283	-0.0263	-0.0096	-0.0047
PI	-0.0441	-0.0957	-0.0576	-0.0009	-0.0017

Table C.2. MCP joint AA parameters

	a_1	a_2	a_3	a_4	a_5
FDP	0.0000	0.0000	-0.0019	-0.0009	-0.0011
FDS	0.0000	0.0000	-0.0043	-0.0006	-0.0012
EIP	0.0000	0.0000	0.0084	0.0035	-0.0021
EDC	0.0000	0.0000	0.0033	0.0016	-0.0001
LUM	0.0000	0.0000	-0.0066	-0.0076	0.0054
DI	0.0000	0.0000	-0.0066	-0.0081	0.0064
PI	0.0000	0.0000	0.0067	0.0054	-0.0057

Table C.3. PIP joint FE parameters

	a_1	a_2	a_3	a_4	a_5
FDP	-0.0100	-0.0270	-0.0235	-0.0058	-0.0071
FDS	-0.0015	-0.0066	-0.0094	-0.0044	-0.0063
EIP	0.0012	0.0027	0.0001	-0.0039	0.0011
EDC	-0.0040	-0.0117	-0.0123	-0.0070	0.0014
LUM	-0.0019	-0.0038	-0.0034	-0.0042	-0.0002
DI	0.0000	0.0000	0.0000	0.0000	0.0000
PI	0.0078	0.0207	0.0147	-0.0006	0.0010

Table C.4. DIP joint FE parameters

	a_1	a_2	a_3	a_4	a_5
FDP	0.0028	0.0033	-0.0012	-0.0032	-0.0053
FDS	0.0000	0.0000	0.0000	0.0000	0.0000
EIP	0.0123	0.0252	0.0132	-0.0005	0.0009
EDC	0.0075	0.0131	0.0030	-0.0039	0.0008
LUM	0.0087	0.0152	0.0071	-0.0002	0.0002
DI	0.0000	0.0000	0.0000	0.0000	0.0000
PI	0.0169	0.0353	0.0202	0.0004	0.0003

Table C.5. CMC joint FE parameters

	a_1	a_2	a_3	a_4	a_5
FPL	-0.2793	0.0658	0.0274	-0.0039	-0.0145
FPB	-0.1995	0.0702	0.0178	-0.0052	-0.0134
EPL	0.0505	-0.0444	0.0249	-0.0040	0.0082
EPB	-0.0146	-0.0151	0.0274	-0.0030	0.0130
APL	-0.0912	0.0078	0.0230	-0.0024	0.0069
APB	0.0193	-0.0071	0.0044	0.0030	-0.0039
ADPt	0.2422	-0.2343	0.0896	-0.0090	-0.0367
ADPo	-0.1929	-0.0934	0.1079	-0.0137	-0.0270
OPP	-0.0083	-0.0006	0.0068	0.0003	-0.0129

Table C.6. CMC joint AA parameters

	a_1	a_2	a_3	a_4	a_5
FPL	0.1874	0.0369	-0.0300	-0.0085	-0.0006
FPB	-0.1261	0.0027	0.0268	-0.0081	-0.0105
EPL	0.2196	-0.0072	-0.0570	0.0006	0.0093
EPB	0.0322	-0.0053	-0.0106	0.0022	-0.0032
APL	-0.1522	0.0204	0.0357	-0.0055	-0.0105
APB	-0.2854	-0.0284	0.0475	-0.0009	-0.0162
ADPt	0.5416	0.2298	-0.1243	-0.0632	0.0203
ADPo	0.1201	0.1022	-0.0759	-0.0405	0.0169
OPP	-0.0487	0.0277	-0.0005	-0.0151	-0.0048

Table C.7. MP joint FE parameters

	a_1	a_2	a_3	a_4	a_5
FPL	0.0232	0.0500	0.0305	-0.0041	-0.0139
FPB	0.0162	0.0433	0.0196	-0.0088	-0.0090
EPL	-0.0175	-0.0255	-0.0078	-0.0023	0.0086
EPB	0.0009	0.0036	0.0048	0.0010	0.0086
APL	0.0000	0.0000	0.0000	0.0000	0.0000
APB	0.0058	0.0147	0.0048	-0.0053	-0.0026
ADPt	0.0192	0.0418	0.0153	-0.0106	-0.0096
ADPo	0.0089	0.0271	0.0127	-0.0092	-0.0081
OPP	0.0000	0.0000	0.0000	0.0000	0.0000

Table C.8. MP joint AA parameters

	a_1	a_2	a_3	a_4	a_5
FPL	-0.0065	0.0042	-0.0045	-0.0131	0.0001
FPB	0.0327	0.0209	-0.0058	-0.0181	-0.0087
EPL	-0.0261	0.0000	0.0016	-0.0017	0.0044
EPB	-0.0588	-0.0042	0.0030	-0.0007	-0.0014
APL	0.0000	0.0000	0.0000	0.0000	0.0000
APB	-0.2417	0.0042	0.0295	-0.0141	-0.0113
ADPt	0.1110	-0.0543	-0.0412	-0.0050	0.0060
ADPo	0.2286	0.0711	-0.0462	-0.0125	0.0040
OPP	0.0000	0.0000	0.0000	0.0000	0.0000

Table C.9. IP joint FE parameters

	a_1	a_2	a_3	a_4	a_5
FPL	-0.0010	0.0000	0.0019	-0.0014	-0.0087
FPB	0.0000	0.0000	0.0000	0.0000	0.0000
EPL	0.0030	0.0028	-0.0054	-0.0052	0.0041
EPB	0.0000	0.0000	0.0000	0.0000	0.0000
APL	0.0000	0.0000	0.0000	0.0000	0.0000
APB	0.0000	0.0000	0.0000	0.0000	0.0000
ADPt	0.0000	0.0000	0.0000	0.0000	0.0000
ADPo	0.0000	0.0000	0.0000	0.0000	0.0000
OPP	0.0000	0.0000	0.0000	0.0000	0.0000

List of Publications

- Refereed Journal Papers -

1. **Atsutoshi Ikeda**, Yuichi Kurita, and Tsukasa Ogasawara, "Biomechanical Analysis of Subjective Pinching Effort Using the Tendon Skeletal Model", *Journal of the Robotics Society of Japan*, Vol. 28, No. 2, pp. 191-199, 2010 (in Japanese).

2. **Atsutoshi Ikeda**, Yuichi Kurita, Jun Ueda, Yoshio Matsumoto, and Tsukasa Ogasawara, "Grip force control of the elastic body based on contact surface eccentricity during the incipient slip", *The Journal of the Robotics Society of Japan*, Vol. 23, No. 3, pp.65-71, 2005 (in Japanese).

3. **Atsutoshi Ikeda**, Yuichi Kurita, Jun Ueda, and Tsukasa Ogasawara, "Development of a compact pointing device utilizing the fingerprint deformation during the incipient slip", *Journal of Information Processing Society of Japan*, Vol. 45, No. 7, pp. 1769-1778, 2004 (in Japanese).

4. Jun Ueda, **Atsutoshi Ikeda**, and Tsukasa Ogasawara, "Grip-force Control of an Elastic Object by Vision-based Slip Margin Feedback during the Incipient Slip", *IEEE Transactions on Robotics*, Vol. 21, No. 6, pp.1139-1147, 2005.

5. Yuichi Kurita, **Atsutoshi Ikeda**, Jun Ueda, and Tsukasa Ogasawara, "A Fingerprint Pointing Device Utilizing the Deformation of the Fingertip during the Incipient Slip", *IEEE Transactions on Robotics*, Vol. 21, No. 5, pp.801-811, 2005.

- Refereed International Conference Proceedings Papers -

1. **Atsutoshi Ikeda**, Yuichi Kurita, and Tsukasa Ogasawara, "A Tendon Skeletal Finger Model for Evaluation of Pinching Effort", *Proceedings of 2009 IEEE/RSJ International Conference on Intelligent Robots and Systems (IEEE IROS 2009)*, pp. 3691-3696, St. Louis, MO, USA, October, 2009.

2. **Atsutoshi Ikeda**, Yuichi Kurita, and Tsukasa Ogasawara, "Evaluation of Pinching Effort by a Tendon-Driven Robot Hand", *Proceedings of 2009 IEEE International Conference on Robotics and Automation (IEEE ICRA 2009)*, pp. 3437-3442, Kobe, Japan, May, 2009.

3. **Atsutoshi Ikeda**, Yuichi Kurita, and Tsukasa Ogasawara, "Pinching Motion Evaluation using Human like Sensing Device", *Proceedings of Joint 4th International Conference on Soft Computing and Intelligent Systems and 9th International Symposium on advanced Intelligent Systems (SCIS & ISIS 2008)*, pp. 1135-38, Nagoya, Japan, September, 2008.

4. **Atsutoshi Ikeda**, Yuichi Kurita, Jun Ueda, Yoshio Matsumoto, and Tsukasa Ogasawara, "Grip Force Control for an Elastic Finger using Vision-based Incipient Slip Feedback", *Proceedings of 2004 IEEE/RSJ International Conference on Intelligent Robots and Systems (IROS 2004)*, pp. 810-815, Sendai, September, 2004.

5. Yuichi Kurita, **Atsutoshi Ikeda**, Takeshi Tamaki, Kazuyuki Nagata, and Tsukasa Ogasawara, "Haptic Augmented Reality Interface using the Real Force Response of an Object", *The 16th ACM Symposium on Virtual Reality Software and Technology (VRST 2009)*, pp. 83-86, Kyoto, Japan, November, 2009.

6. Yuichi Kurita, Yasuhiro Ono, **Atsutoshi Ikeda**, and Tsukasa Ogasawara, "Human-sized Anthropomorphic Robot Hand with Detachable Mechanism at the Wrist", *Proceedings of 2009 IEEE/RSJ International Conference on Intelligent Robots and Systems (IEEE IROS 2009)*, pp. 2271-2276, St. Louis, MO, USA, October, 2009.

7. Yuichi Kurita, Takehiro Onoue, **Atsutoshi Ikeda**, and Tsukasa Ogasawara, "Biomechanical Analysis of Subjective Pinching Effort Based on Tendon-Skeletal Model", *The 31st Annual International Conference of the IEEE Engineering in Medicine and Biology Society (IEEE EMBC 2009)*, pp. 5231-5234, Minnesota, USA, September, 2009.

8. Yuichi Kurita, **Atsutoshi Ikeda**, Jun Ueda, Yoshio Matsumoto, and Tsukasa

Ogasawara, "A Novel Pointing Device Utilizing the Deformation of the Fingertip", *Proceedings of the 2003 IEEE/RSJ International Conference on IntelligentRobots and Systems (IROS 2003)*, pp. 13-18, Las Vegas, USA, October, 2003.

- Japanese Conference Proceedings Papers -

1. **Atsutoshi Ikeda**, Yuichi Kurita, and Tsukasa Ogasawara, "Quantitative Evaluation System of Product Usability Based on Muscle Activity Margin", *In Proceedings of the 15th Robotics Symposia*, 3B3, 2010.

2. **Atsutoshi Ikeda**, Takehiro Onoue, Yuichi Kurita, and Tsukasa Ogasawara, "Influence of the Finger Posture on the Subjective of Pinching Effort", *In Proceedings of JSME Robotics and Mechatronics Conference 2009 (ROBOMEC2009)*, 1A1-M02, 2009.

3. **Atsutoshi Ikeda**, Yuichi Kurita, and Tsukasa Ogasawara, "Tendon Force Sensing for the Quantification of Pinching Effort", *In Proceedings of the 14th Robotics Symposia*, 4D2, 2009.

4. **Atsutoshi Ikeda**, Yuichi Kurita, and Tsukasa Ogasawara, "Measurement of Pinching Motion by a Robot Hand for the Quantification of Pinching Facility", *In Proceedings of the 26th Annual Conference of the Robotics Society of Japan*, 1E2-02, 2008.

5. **Atsutoshi Ikeda**, Yuichi Kurita, and Tsukasa Ogasawara, "Measurement of Pinching Motion for the Quantification of Pinching Facility", *In Proceedings of JSME Robotics and Mechatronics Conference 2008 (ROBOMEC2008)*, 1P1-A11, 2008.

6. **Atsutoshi Ikeda**, Yuichi Kurita, Jun Ueda, Yoshio Matsumoto, and Tsukasa Ogasawara, "Grip Force Control of an Elastic Body Based on Contact Surface Eccentricity During the Incipient Slip", *In Proceedings of JSME Robotics and Mechatronics Conference 2004 (ROBOMEC2004)*, 1A1-H35, 2004.

7. **Atsutoshi Ikeda**, Yuichi Kurita, Jun Ueda, Yoshio Matsumoto, and Tsukasa Ogasawara, "Grip Force Control of the Elastic Body Utilising the Incipient Slip Sensor", *In Proceedings of the 4th Annual Conference of SICE System Integration Divsion of Japan (SI2008)*, pp.424-425, 2003.

8. **Atsutoshi Ikeda**, Yuichi Kurita, Jun Ueda, and Tsukasa Ogasawara, "Development of a Novel Pointing Device Using the Fingertip Deformation -Analysis of the Fingertip Deformation in the Sliding Motion-", *In Proceedings of the 21th Annual Conference of the Robotics Society of Japan*, 3F18, 2003.

9. **Atsutoshi Ikeda**, Yuichi Kurita, Jun Ueda, and Tsukasa Ogasawara, "Development of a New Pointing Device Utilizing Deformation of Fingerprint Images", *In Proceedings of JSME Robotics and Mechatronics Conference 2003 (ROBOMEC2003)*, 1A1-3F-B4, 2003.

10. Kenta Mukai, **Atsutoshi Ikeda**, Yuichi Kurita, Mitsunori Tada, Takashi Maeno, and Tsukasa Ogasawara, "System Identification of Human Grip Force Control Based on Slip and Force", *In Proceedings of the 10th Annual Conference of SICE System Integration Divsion of Japan (SI2009)*, pp. 433-436, 2009.

11. Yuichi Kurita, **Atsutoshi Ikeda**, Atsushi Sobue, and Tsukasa Ogasawara, "Applications of the Acoustic Information in the Task Achievement and the Water Volume Estimation by a Robot Hand", *In Proceedings of the 30th Meeting of Special Interest Group on AI Challenges*, pp. 50-55, 2009.

12. Yuichi Kurita, Atsushi Sobue, **Atsutoshi Ikeda**,and Tsukasa Ogasawara, "Water volume estimation in a glass by a flicking motion based on the glass harp acoustics", *In Proceedings of the 27th Annual Conference of the Robotics Society of Japan*, 1A3-04, 2009.

13. Takeshi Tamaki, **Atsutoshi Ikeda**, Yuichi Kurita, Kazuyuki Nagata, and Tsukasa Ogasawara, "Haptic Augmentation Utilizing the Force Response of a Real Object", *In Proceedings of the 14th Annual Conference of the Virtual Reality Society of Japan*, 1A2-5, 2009.

14. Yuichi Kurita, Yasuhiro Ono, **Atsutoshi Ikeda**, and Tsukasa Ogasawara, "Development of a Human-sized Multifingered Hand with Detachable Wrist", *In Proceedings of JSME Robotics and Mechatronics Conference 2009 (ROBOMEC2009)*, 2A2-B11, 2009.

15. Takeshi Tamaki, **Atsutoshi Ikeda**, Yuichi Kurita, and Tsukasa Ogasawara, "Rheology-based Posture Control of a Multi-link Robot", *In Proceedings of JSME Robotics and Mechatronics Conference 2009 (ROBOMEC2009)*, 2P1-E06, 2009.

16. Yasuhiro Ono, **Atsutoshi Ikeda**, Yuichi Kurita, and Tsukasa Ogasawara, "Development of Multi Fingered Hand with Detachable Wrist", *In Proceedings of the 9th Annual Conference of SICE System Integration Divsion of Japan (SI2008)*, 1H1-1, 2008.

17. Atsushi Sobue, **Atsutoshi Ikeda**, Yuichi Kurita, and Tsukasa Ogasawara, "Microphone-gripper for Task Achievement Evaluation", *In Proceedings of the 26th Annual Conference of the Robotics Society of Japan*, 1K3-06, 2008.

18. Yutaka Ishida, **Atsutoshi Ikeda**, Jun Ueda, Yoshio Matsumoto, and Tsukasa Ogasawara, "Grip-force Control of NAIST-Hand Using Slip Margin Feedback", *In Proceedings of the 22th Annual Conference of the Robotics Society of Japan*, 1J35, 2004.

19. Jun Ueda, **Atsutoshi Ikeda**, Yuichi Kurita, and Tsukasa Ogasawara, "Development of a Novel Pointing Device Utilizing the Fingertip Deformation", *In Proceedings of 2003 Human Interface Symposium*, pp. 251-254, 2003.

20. Jun Ueda, **Atsutoshi Ikeda**, Kenji Shirae, Hiroshi Takemura, Tsukasa Ogasawara, and Shingo Oda, "Analysis of Human Walking and Motion Using Lateral Rotational Moment of Hip Joints", *In Proceedings of the Welfare Engineering Symposium 2003*, pp. 85-88, 2003.

21. Jun Ueda, **Atsutoshi Ikeda**, Kenji Shirae, Hiroshi Takemura, Tsukasa Ogasawara, and Shingo Oda, "Characteristics of 'Namiashi' Walk: Trunk-twistless Motion using External Rotational Moment of Hip Joints", *In Pro-*

ceedings of the 21th Annual Conference of the Robotics Society of Japan, 2J27, 2003.

- Awards -

1. **Atsutoshi Ikeda**, "Pinching Motion Evaluation using Human like Sensing Device", *Young Researcher Award from SCIS*, 2008.

- Patents -

1. Yuichi Kurita, **Atsutoshi Ikeda**, Tsukasa Ogasawara, "Sensitivity and technique evaluation method and system", *Japanese Patent Application No. 2010-001597*, 2010.

2. Yuichi Kurita, **Atsutoshi Ikeda**, Yasuhiro Ono, Tsukasa Ogasawara, "Robot hand", *Japanese Patent Application No. 2008-308303, PCT/JP2009/70312*, 2009.

3. Jun ueda, Tsukasa Ogasawara, **Atsutoshi Ikeda**, Masahiro Kondo, "Robot hand", *Japanese Patent Application No. 2003-303022*, 2003.

4. Jun ueda, Tsukasa Ogasawara, **Atsutoshi Ikeda**, Yuichi Kurita, "Pointing device", *Japanese Patent Application No. 2003-051530*, 2003.